AGU PUBLICATIONS

Tectonics

RESEARCH ARTICLE
10.1002/2016TC004448

Special Section:
Orogenic cycles: from field observations to global geodynamics

Changing patterns of exhumation and denudation in front of an advancing crustal indenter, Tauern Window (Eastern Alps)

S. Favaro[1], M. R. Handy[1], A. Scharf[1,2], and R. Schuster[3]

[1]Department of Earth Sciences, Freie Universität Berlin, Berlin, Germany, [2]Now at Department of Earth Science, Sultan Qaboos University, Muscat, Oman, [3]Geologische Bundesanstalt, Vienna, Austria

Key Points:
- Post-nappe folding during indentation of orogenic crust in the Tauern Window was transitional to orogen-parallel extension
- At the leading edge of an indenting block, initial strike-slip faulting during early indentation was transitional to extension
- 60–70% of denudation was due to post-nappe folding and erosion, the rest to coeval exhumation and erosion during normal faulting

Supporting Information:
- Supporting Information S1

Correspondence to:
M. R. Handy
mark.handy@fu-berlin.de

Citation:
Favaro, S., M. R. Handy, A. Scharf, and R. Schuster (2017), Changing patterns of exhumation and denudation in front of an advancing crustal indenter, Tauern Window (Eastern Alps), *Tectonics*, *36*, 1053–1071, doi:10.1002/2016TC004448.

Received 20 DEC 2016
Accepted 29 APR 2017
Accepted article online 6 MAY 2017
Published online 5 JUN 2017

Abstract The changing shape of indenting crustal blocks during northward motion of the Adriatic microplate induced migration of Miocene doming and orogen-parallel extension of orogenic crust in the Tauern Window. New structural and kinematic data indicate that initial shortening of the Penninic nappe pile in the Tauern Window by upright folding and strike-slip faulting was transitional to coeval north-south shortening and east-west extension; the latter was accommodated by normal faulting at the eastern and western margins of the window. Retrodeforming these post-nappe structures in map view yields a map-view reconstruction of the orogenic crust back to 30 Ma, including the onset of pronounced indentation at ~21 Ma. This model supports the notion that indentation involved approximately equal amounts of north-south shortening and orogen-parallel stretching and extrusion toward the Pannonian Basin, as measured from the indenter tip to the European foreland in the north and Austroalpine units in the east. Comparison of areal denudation of the orogenic crust before and after indentation indicates that erosion associated with upright folding was the primary agent of denudation, whereas extensional unroofing and limited erosion along normal faults at the eastern and western ends of the Tauern Window accounted for only about a third of the total denudation.

1. Introduction

Indentation of orogenic lithosphere by an impinging tectonic plate changes the dynamic and kinematic boundary conditions of the orogenic wedge, triggering rapid exhumation by doming, normal faulting, and erosion [*Johnson*, 2002], and in some cases inducing orogen-parallel escape [e.g., *Tapponnier et al.*, 1986]. In the Alpine chain, the leading edge of the Adriatic Microplate (Southern Alpine crust) is divided into western and eastern blocks by the Giudicarie Belt. Thus, the response of the thickened European lithosphere to indentation varies along strike of the Alpine orogen: in the central Alps, i.e., west of the Giudicarie Belt and the Brenner Normal Fault (Figure 1), indentation triggered backfolding and thrusting of the European crust [e.g., *Argand*, 1924; *Dal Piaz*, 1999] above a wedge of Adriatic lower crust [e.g., *Schmid et al.*, 2004; *Rosenberg and Kissling*, 2013], whereas in the Eastern Alps, it involved doming, extensional exhumation, and eastward lateral escape of Austroalpine units and orogenic crust exposed in the Tauern Window (Figure 1) [e.g., *Ratschbacher et al.*, 1991b; *Selverstone*, 2004; *Horváth et al.*, 2006; *Scharf et al.*, 2013a].

The Tauern Window in the Eastern Alps (Figure 1) is well suited to study patterns of exhumation and denudation during indentation due to the three-dimensional exposure of deeply subducted and exhumed European crust in front of the Adriatic indenter. Denudation, i.e., the removal of rock from above exhuming crust [*England and Molnar*, 1990], can be broken down into contributions from erosion and tectonic unroofing; the latter involves normal faults which displace crust laterally in their hanging walls while exhuming orogenic crust in their footwalls (e.g., the Brenner and Katschberg normal faults in Figure 1 [*Behrmann*, 1988; *Selverstone*, 1988; *Genser and Neubauer*, 1989; *Fügenschuh et al.*, 1997; *Scharf et al.*, 2013a]). The mechanisms of exhumation vary along strike of the Tauern Window: the central part shows little or no orogen-parallel extension and preserves subduction-related fabrics, whereas the eastern and western ends of the window display kilometer-scale upright folds and extensional shear zones that deform all accretionary structures and overprint Oligocene Barrovian-type amphibolite-facies metamorphism [*Kurz et al.*, 1998; *Scharf et al.*, 2013a] of the so-called "Tauernkristallisation" [*Sander*, 1911]. Interestingly, the distribution of cooling ages in the Tauern Window indicates that rapid exhumation and subsequent cooling in Miocene time may have

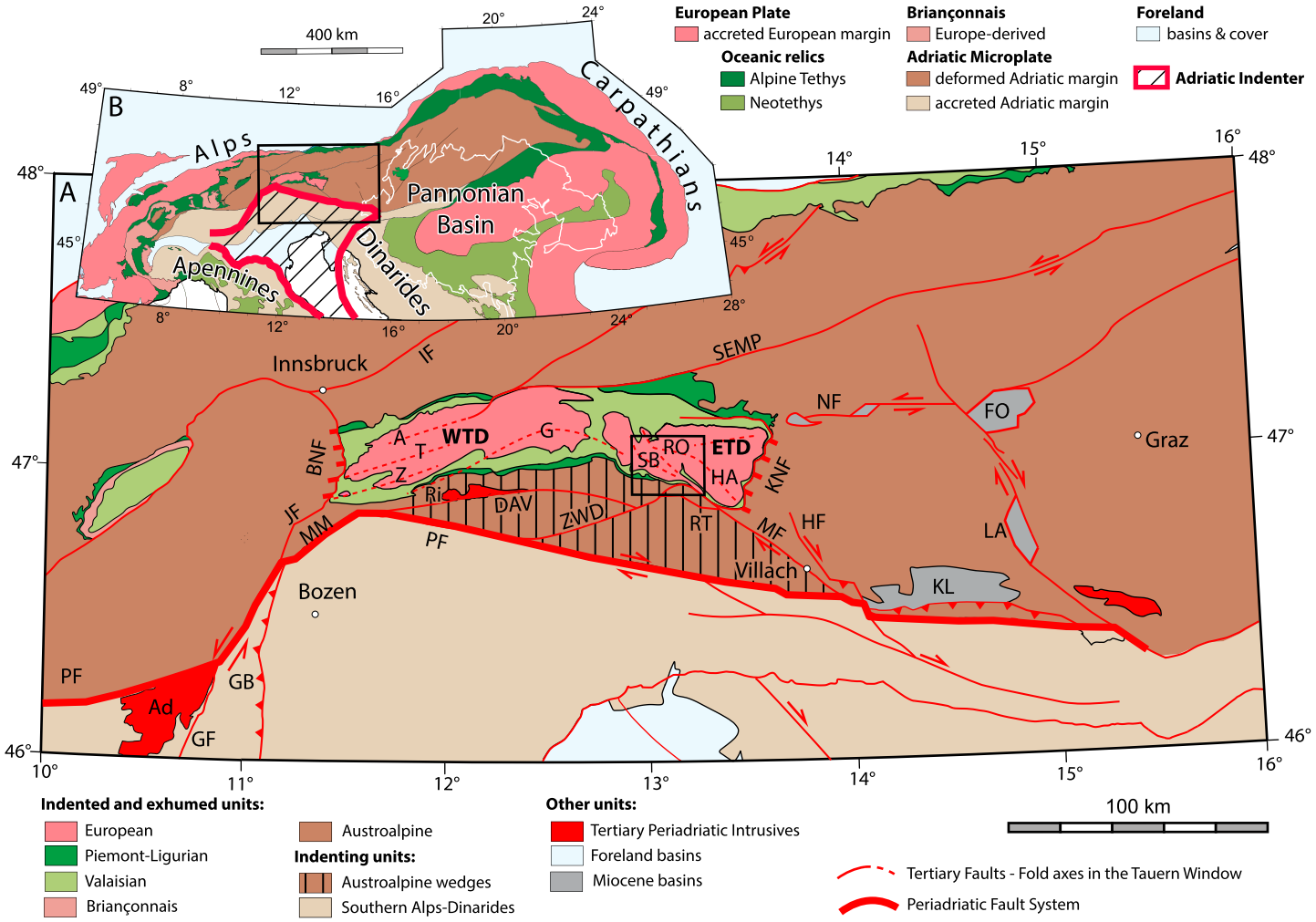

Figure 1. Tectonic map of the Eastern Alps showing units of indenting Adriatic and European plates with intervening oceanic units of Alpine Tethys as modified from *Scharf et al.* [2013a]. The box indicates area in Figure 2. Faults and shear zones: BNF, Brenner Normal Fault; DAV, Defereggen Anterselva Valles Fault; GB, Giudicarie Belt (includes Giudicarie Fault, GF); HF, Hochstuhl Fault; IF, Inntal Fault; JF, Jaufen Fault; KNF, Katschberg Normal Fault; MF, Mölltal Fault; MM, Meran Mauls Fault; NF, Niedere Tauern Southern Fault; PF, Periadriatic Fault; RT, Ragga-Teuchel Fault; SEMP, Salzach-Ennstal-Mariazell-Puchberg Fault; ZWD, Zwischenbergen-Wöllatratten-Drau Fault. Domes and thrust-belt: A, Ahorn; G, Granatspitz; HA, Hochalm; RO, Romate; SB, Sonnblick; T, Tux; Z, Zillertal. Neogene basins: FO, Fohnsdorf; KL, Klagenfurt; LA, Lavanttal; ETD, Eastern Tauern Subdome; WTD, Western Tauern Subdome. Periadriatic plutons: Ad, Adamello; Ri, Rieserferner. Inset map shows major units of Alps and Carpathians, and the major continents and oceans involved in collision (Europe, Adria). The white line delimits the Plio-Pleistocene fill in the Pannonian Basin.

begun earlier in the eastern than the western part [*Luth and Willingshofer*, 2008; *Scharf et al.*, 2013a]. If so, rapid exhumation varied in time as well as in space in front of the Adriatic indenter. The pattern of exhumation and cooling through time is crucial in the light of an ongoing controversy in the Eastern Alps of whether denudation involved primarily upright folding and erosion [*Rosenberg et al.*, 2007] or whether tectonic unroofing in the footwalls of the normal faults [*Frisch et al.*, 1998, 2000; *Linzer et al.*, 2002] were responsible for the exposure of subducted European crust.

This paper presents new structural and kinematic data from the southeastern part of the Tauern Window, documenting for the first time that the kinematics of faulting along the leading edge of the indenting blocks are opposite to that of mylonitic shearing in the adjacent exhuming orogenic crust. This striking difference in kinematics reflects the contrasting geometries and rheologies of indenting (brittle) and indented (mylonitic) crust during coeval north-south shortening and east-west orogen-parallel escape. Using structural and thermochronological data for the entire Tauern Window, we provide a map-view reconstruction of post-Eocene crustal motion in the Eastern Alps indicating that denudation of the Tauern Window during indentation is not due primarily to extensional unroofing but to upright folding and erosion.

2. Geological Setting

The Tauern Window exposes accreted basement and cover of the originally downgoing European crust, including remnants of Alpine Tethys. These accreted and exhumed units are exposed beneath remains of the upper Adriatic plate which frame the Tauern Window (Austroalpine units in Figure 1). The Austroalpine units exposed just south of the Tauern Window formed indenting blocks or wedges (Rieserferner and Drau-Möll blocks or wedges [*Scharf et al.*, 2013a; *Favaro et al.*, 2015]) and are separated from the Southern Alps by the Periadriatic Fault (Figure 1). The Southern Alps form the leading edge of the Adriatic Indenter, i.e., that part of the Adriatic Microplate which indented the orogenic crust [*Handy et al.*, 2010].

During Adria-Europe convergence, the lower plate units in the Tauern Window experienced deformation and metamorphism associated with accretion and subduction (D_1), exhumation (D_2 and D_3), collision (D_4), and indentation (D_5). The use of D followed by a number merely indicates the relative age of structures (1 oldest to 5 youngest) as constrained by overprinting relations and does not mean that these structures formed during distinct events at the scale of the orogen; in fact, they probably developed more or less continuously from Late Cretaceous to Miocene time [*Schmid et al.*, 2013]. The age of D_5 structures related to exhumation varies across and along the Tauern Window, creating a pattern which can be related to the progressive changes in the shape and kinematics of the indenting blocks.

The ends of the Tauern Window comprise two thermal and structural domes (D_5), the Eastern and Western Tauern domes (ETD and WTD), which expose the deepest structural units. These domes are doubly plunging, upright antiforms that overprint duplex structures formed during north-directed collisional nappe stacking (D_4). In the ETD, a roof thrust separates kilometer-thick basement slices below (D_4, Venediger Nappe System) from an isoclinally D_3-folded thrust (D_2) above. This folded thrust is the oldest structure in the area and emplaced Alpine Tethyan ophiolites (Glockner Nappe System [e.g., *Pestal et al.*, 2009]) onto a distal unit of the European margin (Modereck Nappe System [*Schmid et al.*, 2013]). The units above the roof thrust have a composite S2-3 foliation that is locally overprinted by upright folds and shear zones related to indentation (D_5). All pre-indentational structures (pre-D_5) are overprinted by the Tauernkristallisation thermal event [*Sander*, 1911; *Hoinkes et al.*, 1999] that is marked by concentric isograds [*Oberhänsli et al.*, 2004] and isotemperature lines [*Scharf et al.*, 2013b] outlining amphibolite-facies conditions in the cores of the ETD and WTD. When combined with thermochronology discussed below, these overprinting relationships place important constraints on the pattern of exhumation of accreted units during indentation.

3. Structures and Kinematics Related to Indentation in the Eastern Tauern Dome

A NW-SE striking synform (the Mallnitz Synform) divides the ETD into two subdomes, the Sonnblick and Hochalm subdomes (Figure 2). This synform contains the infolded remains of the D_4 roof thrust mentioned above. The Sonnblick Subdome (Figure 2) ("Sonnblick Walze" of *Exner* [1948]) thins drastically at its southeastern end, forming an elongate gneiss lamella only 50–70 m thick in map view (Figure 2) ("Sonnblick Lamella" of *Exner* [1964]). The Hochalm Subdome is also thinned and truncated along its eastern margin by a top-SE, crustal-scale normal fault (the Katschberg Normal Fault (KNF) [*Genser and Neubauer*, 1989]) which, together with its steep northern and southern mylonitic branches [*Scharf et al.*, 2013a], accommodated E to SE directed orogen-parallel extension (Figure 1).

Figure 2 shows that structures related to nappe stacking and isoclinal folding (D_2–D_4 in black) are modified by postnappe folding and shearing (D_5 structures in red). The intensity of D_5 overprinting increases from NW to SE, parallel to the trace of the Mallnitz Synform as marked by its progressive tightening, from tight (Figure 3, section d) with a subvertical axial plane (Figure 3, sections e–f) to isoclinal with a moderately SW-dipping axial plane (Figure 3, sections a–c). This tightening is accompanied by the development of an axial plane schistosity (Figure 2, domain A) that varies from a spaced schistosity (Figure 2, domain A, and Figure 3, cross sections a–c) to a penetrative mylonitic foliation (Figure 2, domains B and C, and Figure 3, sections d–f) with a subhorizontal to gently SE-plunging stretching lineation (Figure 2, domains A–C) and moderately dipping sinistral shear bands (Figure 2, domain C). The counterclockwise curvature of older D_4 foliations and stretching lineations [*Exner*, 1964, his Plate 3] (Figure 2, domains D and E) into concordance with the D_5 shearing plane, as well as small-scale kinematic indicators (Figure 4c), are consistent

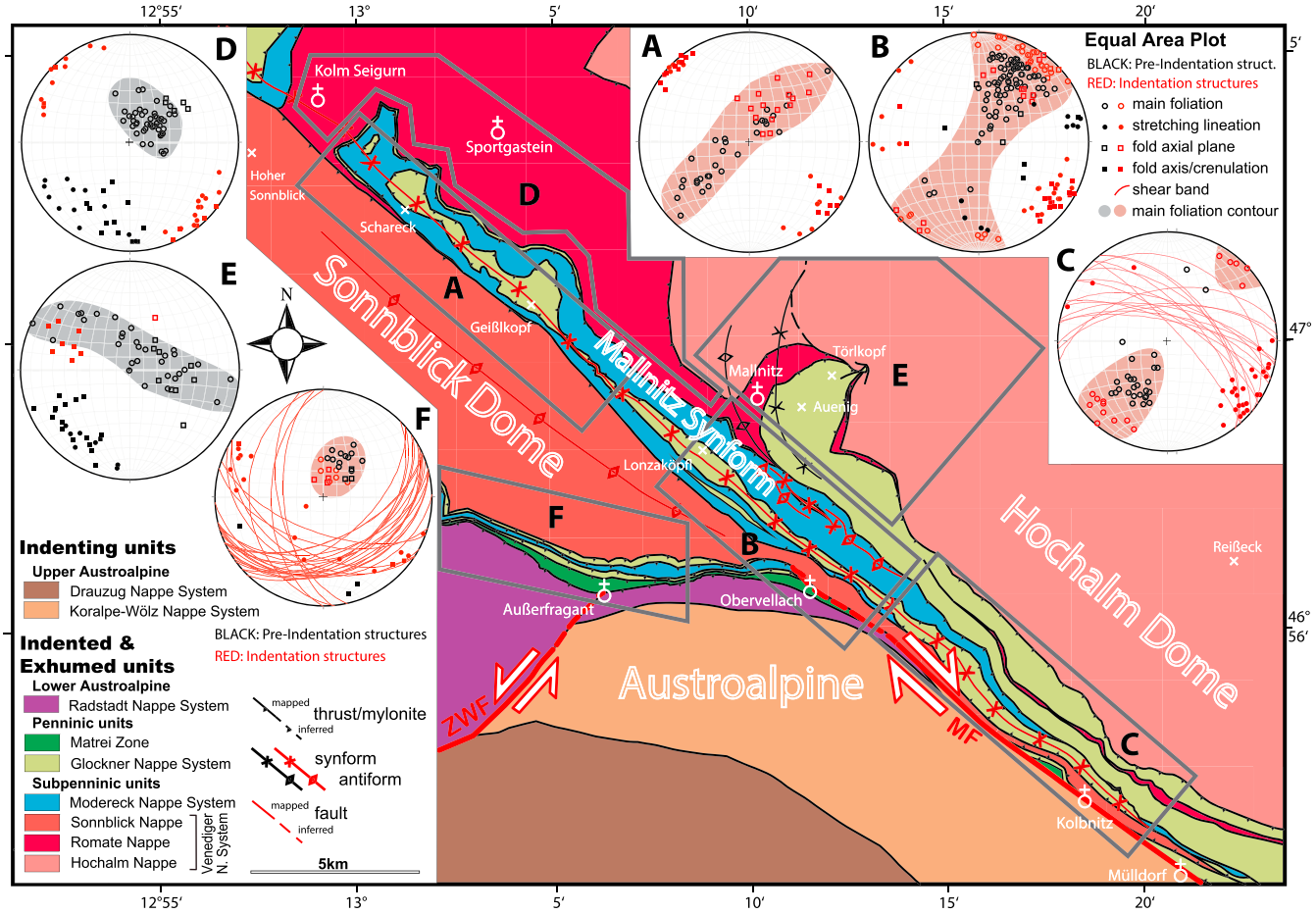

Figure 2. Map of the southeastern Tauern Window showing indenting units of the upper plate (brown) and indented and exhumed units of the lower plate (all other colors). Structural domains A-F with equal-area plots showing orientations of the pre-indentational (black) and indentational structures (red). Brittle faults delimiting the Drau-Möll Block: MF, Mölltal Fault; ZWF, Zwischenberg-Wöllatratten Fault. See legend and text for explanation. The stars are locations of outcrops of brittle fault surfaces at Obervellach and Kolbnitz (section 4 and Figures 5f and 6).

with transpressive sinistral shearing in map view combined with NE-side up exhumation of the Hochalm Subdome. This mylonite belt bends around the southeastern end of the D_5 Hochalm Subdome to become the ductile part of the Katschberg Normal Fault (KNF; Figure 1) or the Katschberg Shear Zone System of *Scharf et al.* [2013a]. The coincidence of tectonic omission of footwall units along the KNF (26 km) with the axial culmination of the Hochalm Subdome indicates that D_5 folding and top-E to -SE extensional shearing along the KNF were coeval [*Scharf et al.*, 2013a] as observed in the footwall of the Brenner Normal Fault at the western end of the Tauern Window [e.g., *Behrmann*, 1988; *Selverstone*, 1988; *Fügenschuh et al.*, 1997].

The Sonnblick Subdome folds a composite S_{4-5} foliation with a pronounced stretching lineation trending parallel to the antiformal axis. Within the subdome, some moderately inclined shear bands with both NW and SE-plunging stretching lineations indicate subvertical flattening beneath the Austroalpine units (domain F in Figure 2). The southern end of the Sonnblick Subdome shows S to SE dipping shear bands indicating extensional exhumation of all Penninic units both above and below the D_4 roof thrust (Figure 2, domain F, and Figure 4a). The Penninic and Subpenninic units in the footwall of this extensional shear zone are severely thinned, such that the previously thrusted and folded Matrei Zone, Glockner, and Modereck Nappe Systems are reduced to only about 500 m of their original ~4 km thickness. A second, later set of shear bands along the south margin of the Sonnblick Subdome near the Sonnblick Lamella accommodated sinistral shearing in map view [*Kurz et al.*, 1996] (Figure 4c). Although the shearing directions of these two sets of shear bands differ (see equal-area plot for domain F in Figure 2), we interpret them to represent a

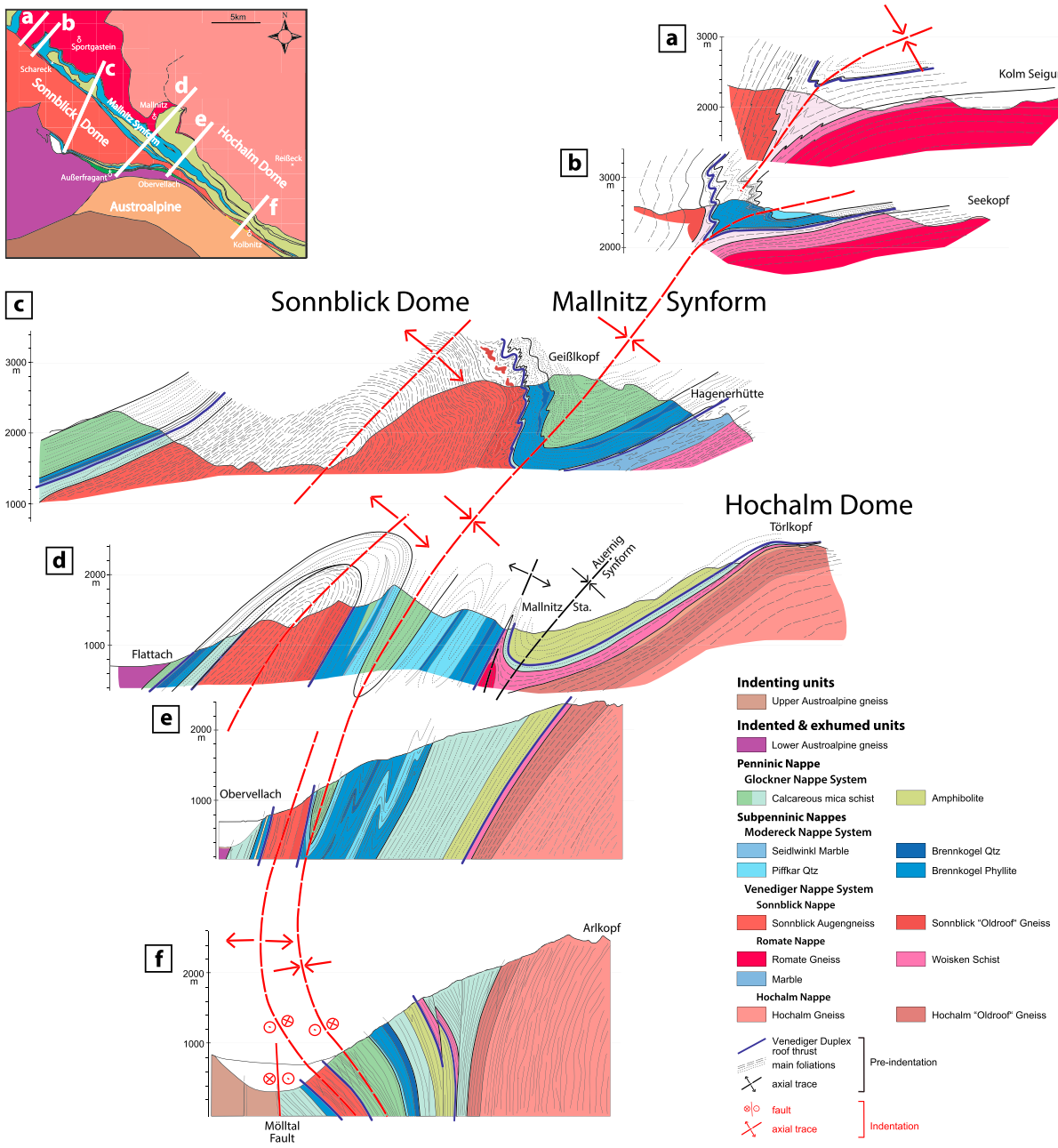

Figure 3. Cross sections of the Mallnitz Synform and adjacent Sonnblick and Hochalm subdomes: (a and b) "Rauris Valley" sections, (c) "Hagener" section, (d) "Mallnitz" section, (e) "Kaponig" section, and (f) "Kolbnitz" section. The red dashed lines represent traces of the F5 axial planes; the black dashed lines indicate main S5 foliation. Older foliations indicated with thin grey lines. Inset shows map of area as in Figure 2. Note in Figure 3f the opposite shear senses of indenting Austroalpine crust along the Mölltal Fault (dextral) and of indented orogenic crust along the steep southern branch of the Katchberg Normal Fault (sinistral) described in the text.

progressive evolution from top-S to -SE extensional shearing to tightening of the Sonnblick Subdome during continuous northward motion of the indenting Drau-Möll Block (see section 5).

Locally, especially in fabric domain A (Figure 2), relics of pre-indentational structures are still preserved, despite the strong D_5 overprint. D_4 fold axes and stretching lineations are preserved only in the late Paleozoic-Mesozoic cover of the Venediger Nappe System and usually plunge to the S and SW. D_4 folds are clearly recognizable because their axial planes strike perpendicular to the D_5 structures and because they face to the NNW, i.e., in the direction of thrusting and nappe stacking (Figure 5a). The main foliation is mylonitic and contains shear bands indicating top-N nappe stacking direction (Figure 5b).

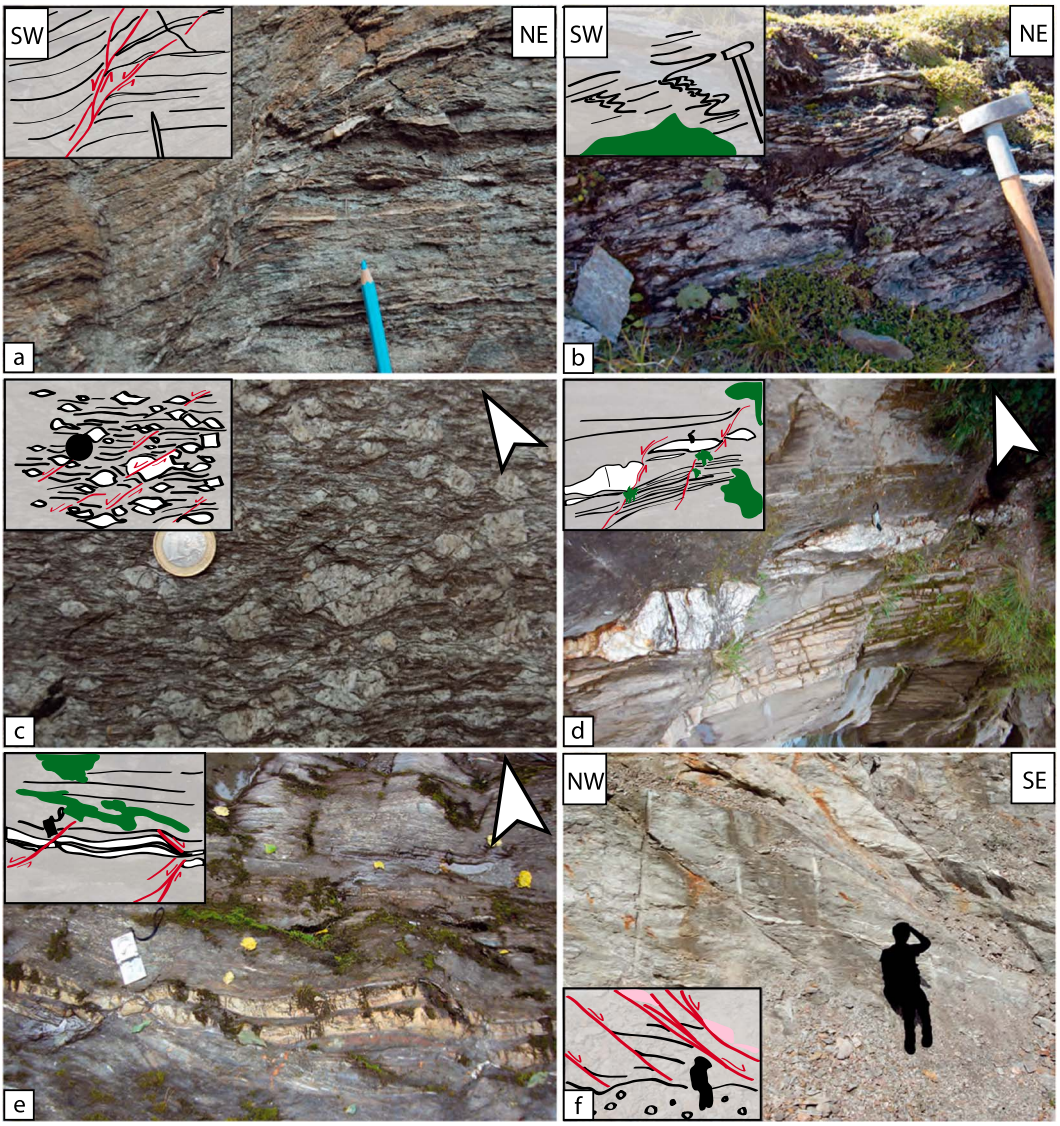

Figure 4. Key structures related to indentation as depicted in domains A–F in Figure 2: (a) top-down-to-SE ductile-brittle shear bands near Außerfragant at the southeastern end of Sonnblick Subdome, domain F; (b) isoclinal D_5 folds deform S_{2-3} in domain A (between Kolm Saigurn and Schareck); (c) augengneiss of the Sonnblick Lamella in map view showing sinistral shear bands offsetting feldspar clasts in domain C (near Kolbnitz); (d) sinistral shear band offsetting quartz vein in map view near Obervellach, domain B; (e) sinistral and dextral shear bands in map view at SE end of Sonnblick Subdome near Obervellach, domain F, indicating flattening; (f) Mölltal Fault with older fault system (indicated in pink) in Lower Austroalpine gneiss oriented parallel to the outcrop surface and offset by top-SSE faults marked in red. These younger faults show top-down-SE drag (Mühldorf, location in Figure 1, first author for scale).

4. Kinematics and Paleostrain Analysis of the Mölltal Fault

The Mölltal Fault bounds the NE side of the Drau-Möll Block (Figure 2, inset). Detailed mapping shows that the best outcrops of cataclasite along the new Tauern railway line occur within Austroalpine units and not directly at the contact between Austroalpine and Penninic units, which anyway is mostly buried beneath Plio-Pleistocene colluvium of the Möll Valley. The lack of coincidence of the Austroalpine-Penninic contact with the best exposed cataclasite suggests that brittle deformation postdated the juxtaposition of Austroalpine and Penninic units, which must have occurred already during Late Cretaceous to Paleogene nappe stacking [e.g., *Kurz et al.*, 2008; *Schmid et al.*, 2013].

Investigation of several fresh exposures along the new Tauern railroad line in the Möll Valley between Obervellach and Spittal a.d. Drau reveals two generations of fault surfaces (Figure 4f): Surfaces aligned

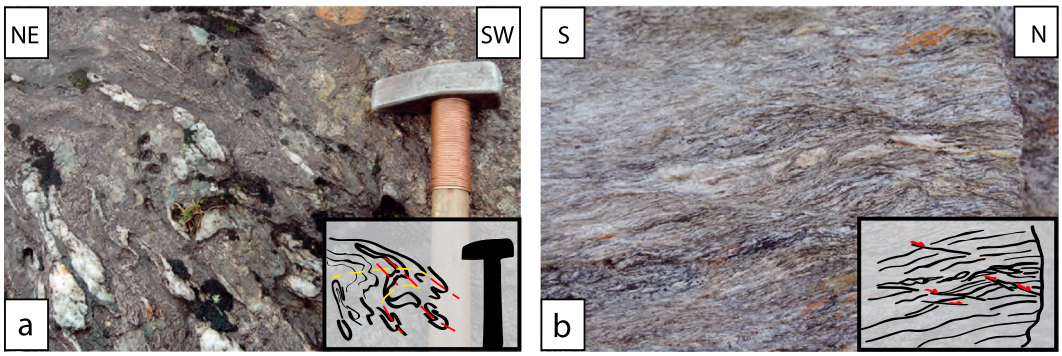

Figure 5. Pictures and sketches of collisional structures beneath the roof thrust in the ETD: (a) F5 folds (red axial plane) deform main foliation (presumably S4) and previously folded quartz veins (yellow F4 axial planes) in late Paleozoic cover of the Sonnblick thrust sheet in fabric domain A; (b) top-N D_4 shear bands in late Paleozoic granitoid at the base of the Romate thrust sheet.in fabric domain D.

subparallel to the valley that carry subhorizontal striations (type 1) are cut by moderately SE dipping surfaces (type 2) that rarely have striations.

The sense of motion on type 1 surfaces is usually sinistral as indicated by tension gashes and more rarely, hematite-bearing slickenfibers exposed along the railway line (criteria of *Petit* [1987]). However, some dextral motion indicators are also present. Type 1 surfaces in the Penninic units along the northeastern side of the Möll Valley, e.g., within the Sonnblick Lamella, display calcite-bearing slickenfibres consistent with dextral strike-slip motion. Thus, there is no clear picture of the sense of shear on the type 1 surfaces; both sinistral and dextral motions are recorded in map view. Unfortunately, there are no overprinting relationships to indicate the relative age of these opposite motion senses. However, dextral motion is consistent with the map-view displacement of Austroalpine nappe contacts by some 26 km [*Linzer et al.*, 2002]. Due to the shallow dip of these contacts, the actual displacement is much less, as discussed in section 5.3. The sense of motion along the moderately dipping type 2, only exposed along the railway line, is more consistent; in both measured outcrops (stars E and F in Figure 6), Riedel shears and dragged schistosity planes indicate that the southeastern block was downthrown with respect to the northwestern block. This is consistent with the sense of motion on the Katchberg Normal Fault.

Four outcrops with a total of 128 measurements were chosen for a paleostrain analysis with the so-called *P-T-B* method (*P*, pressure; *T*, tension; and *B*, intermediate axes): two in Austroalpine units exposed along the railway line (stars C, E, and G and D, F and H in Figure 6), one in the Sonnblick Lamella along the road connecting Obervellach and Mallnitz (star A in Figure 6), and one in the Glockner Nappe System in a creek north of Kolbnitz (star B in Figure 6). In order to perform such an analysis on these fault surfaces, the quality of slip-sense indicators was classified to weight the data (see Table S2 in the supporting information for classification of the data).

The *P-T-B* method is based on the premise that the slip vector and the normal to the fault plane define a plane that contains the maximum and minimum stress axes, $\sigma 1$ and $\sigma 3$. The *P*, *T*, and *B* axes are defined for each measured plane [*Marrett and Allmendinger*, 1990] then calculated for all planes and plotted in an equal-area net, where the average directions of these axes are considered to correspond to the directions of the principal stress axes, $\sigma 1$, $\sigma 2$, and $\sigma 3$. For small increments of strain (i.e., minor slip motions on the fault planes), the *P-T-B* axes coincide exactly with the principal stresses axes. However, measurable displacements are not strictly incremental, so that the *P-T-B* axes often reflect the principal finite strain axes (e_1, e_2, and e_3) rather than the principal axes of the paleostress tensor. For this reason, Table 1 lists the results in terms of the principle finite strain axes. Only fault surfaces with clearly defined dips and dip azimuths and with striations with unequivocal shear sense indicators were used for *P-T-B* analysis with the software WinTensor 3.0.0 [*Delvaux and Sperner*, 2003]. Type 2 fault surfaces were analyzed separately from type 1 surfaces in accordance with the overprinting relationship between these types in all outcrops. In addition, type 1 surfaces that indicate dextral motion were analyzed separately from those with sinistral motion in order to obtain a meaningful result.

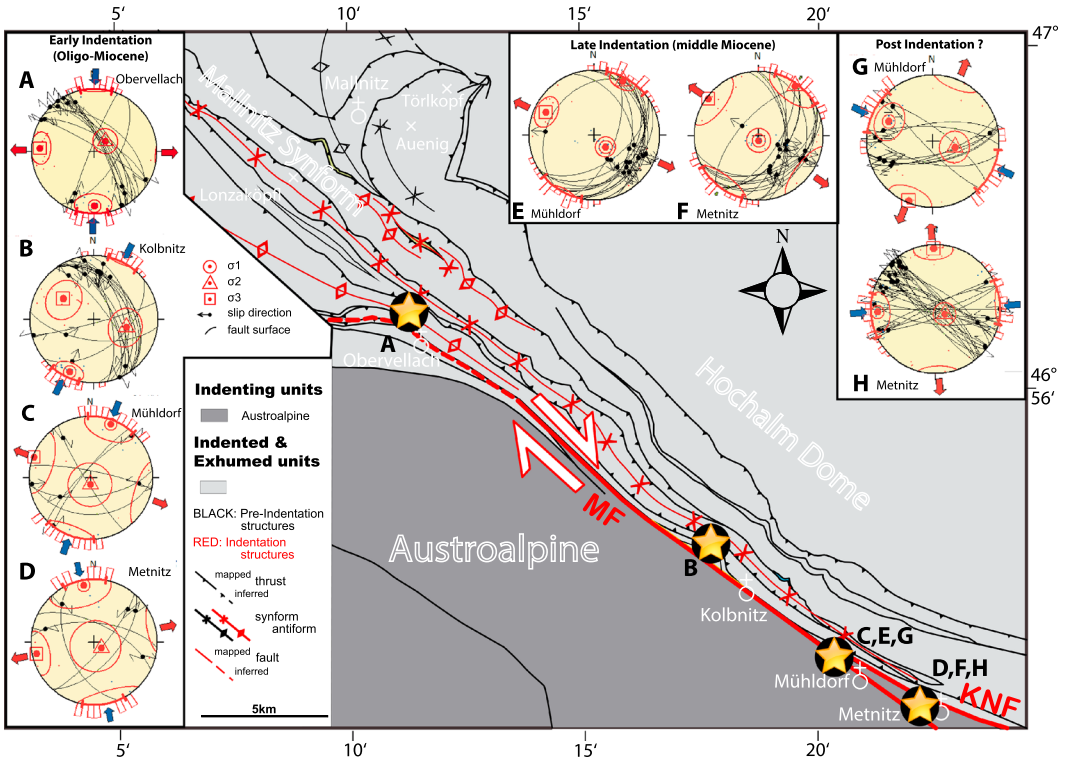

Figure 6. *P-T-B* paleostrain analysis of fault planes in cataclasite along the Mölltal Fault that overprint mylonite of the southern branch of the KNF. (a) Brittle deformation of Sonnblick Lamella near Obervellach; (b) brittle deformation in the Glockner Nappe System near Kolbnitz; (c, e, and g) cataclasites in Lower Austr0alpine Unit, railroad cut near Mühldorf; and (d, f, and h) cataclasites in lower Austroalpine Unit, railroad cut near Metnitz.

The *P-T-B* analysis reveals that type 1 surfaces with dextral motion in the Penninic units accommodated N-S shortening and E-W extension (Figures 6a–6d), which is consistent with dextral shear parallel to the trace of the Mölltal Fault as already proposed by several authors [*Kurz et al.*, 1994; *Kurz and Neubauer*, 1996, and references therein; *Linzer et al.*, 2002]. However, it is opposite to the sinistral shear indicators in the southern mylonitic branch of the KNF bordering the Hochalm Subdome, as documented above and in *Scharf et al.* [2013a]. Most type 1 faults in the Austroalpine units show E-W shortening and N-S extension, and only a

Table 1. Results of Paleostrain Analysis[a]

Cluster	n_t	n	e_1	e_2	e_3	R'	α_w	QR_t	S_{hmax}
a	17	14	13/180	70/049	14/273	1.5 (SS)	15.74	*C*	1 ± 14.7
b	19	15	10/205	46/104	42/304	1.59 (TS)	18.64	*B*	27 ± 13.8
c	6	6	08/020	81/184	02/290	1.56 (SS)	27.17	*D*	020 ± 23.1
d	7	5	09/350	78/130	08/258	1.36 (SS)	28.01	*E*	168 ± 19.7
e	12	10	28/294	62/105	04/202	1.5 (SS)	16.55	*C*	112 ± 20.3
f	32	24	12/267	76/118	07/358	1.5 (SS)	15.01	*C*	87 ± 19.9
g	16	15	69/136	07/028	20/296	0.48 (NF)	11.06	*E*	23 ± 19.5
h	20	15	84/176	05/036	04/306	0.38 (NF)	20.63	*C*	36 ± 23

[a]"Cluster" in the left-hand column refers to a group of measurements at a specific location in the four outcrops (stars in Figures 1 and 2). n_t indicates the total number of measurement; *n* indicates the number of measurements used; e_1, e_2, and e_3 indicate the principle finite strain axes; R' indicates the numerical value of the fault type (0–0.5 = normal fault, 0.5–1.5 = strike-slip, >1.5 = thrust) with end-member fault category in parenthesis (SS, strike-slip; NF, normal fault; TS, thrust); QR indicates the quality rank ranging from *A* (very good) to *E* (very poor) [*Delvaux and Sperner*, 2003] depending on the number of measurements, the average slip deviation angle, the confidence level of the field observation (1, poor to 5, excellent), and the variation of strike orientations within a cluster of measurements., α_w indicates the deviation between observed and theoretical slip directions. S_{hmax} indicates the average strain ratio, i.e., the shape of the finite strain ellipsoid. See Figure 6 for a graphical representation of these results.

few accommodated N-S shortening and E-W extension (Figures 6c and 6d and 6g and h). In contrast, the moderately dipping type 2 surfaces accommodated NE-SW shortening and NW-SE extension (Figures 6e and 6f). Again, this matches the pattern of E to SE directed extension along the KNF.

The dextral type 1 surfaces confirm the overall dextral displacement along the Mölltal Fault as inferred from the map-view offset of Austroalpine units with similar Eo-Alpine histories (e.g., the Koralpe-Wölz Unit [*Linzer et al.*, 2002; *Schuster et al.*, 2004; *Schmid et al.*, 2013]). This dextral motion records the northward motion of the indenting Drau-Möll Block (Figure 2c), whereas the sinistral motion along the steep, southwestern mylonitic margin of the Hochalm Subdome (Figure 3f) reflects ductile extension and exhumation of hot Penninic units in the footwall of the KNF, whose hinge migrated to the southeast, out of the way of the advancing indenter (Figure 7b). This contrasts with previous interpretations in which dextral shear was believed to have affected not just the Mölltal Fault but also the Hochalm and Sonnblick Subdomes, as well as the Mallnitz Synform [*Kurz et al.*, 1994; *Kurz and Neubauer*, 1996].

The sinistral type 1 surfaces indicate shortening and extension directions that do not fit with N-S directed indentation in Miocene time, nor indeed with any other recognizable strain pattern in the area. We therefore suspect that sinistral motion on such surfaces reflects local adjustments along the leading edge of the indenting Drau-Möll Block that are superposed on the overall dextral motion. The type 2 fault surfaces whose motion sense coincides with the extensional direction of the KNF are interpreted to have formed during a late stage of lateral orogenic escape, most likely during or after activity along the KNF, as discussed below.

5. Kinematic Model of Indentation and Tauern Exhumation

We now return to the main question posed in the introduction of how indentation was related to the shortening and lateral orogenic escape recorded in the sections above, and in turn, how these bear on tectonic and erosional denudation. To answer this, we reconstructed the kinematics of indentation of the Eastern Alps in map view back in time (Figure 7), first to the onset of rapid Adriatic indentation of the Eastern Alps at ~21 Ma (Figure 7b), then to the beginning of exhumation of the Alpine orogenic wedge at about 30 Ma (Figure 7a) following break-off of the European slab beneath the Alps [*Davies and von Blanckenburg*, 1995; *Handy et al.*, 2015]. The reader is referred to the supporting information 1 for detailed descriptions of the age and displacements along faults that document the onset of indentation and otherwise form the basis for this reconstruction.

Map-view reconstructions of the Tauern area have been attempted before [*Frisch et al.*, 1998; *Linzer et al.*, 2002], but the model below differs in employing improved estimates of displacement on the Brenner and Katschberg Normal Faults, as well as on the faults delimiting the triangular Austroalpine subindenters north of the PF. This has important consequences for determining the origins and amounts of denudation. Of course, a truly 3-D approach would be desirable given the 3-D response of the orogenic crust to indentation, but this is obviated by the lack of subhorizontal markers (e.g., the Moho) for tracking changes in crustal thickness and vertical motion back in time.

5.1. Boundary Conditions and Assumptions

Several assumptions were made regarding the initial and final configurations of the crust and the conservation of crustal volume and mass during indentation. The eastern block of the indenting Adriatic Microplate comprises the eastern Southern Alps, i.e., the part of the Alps bounded by the Periadriatic Fault to the north and the Giudicarie Belt to the west (Figure 1). The northern leading edge of this Southern Alpine indenter maintained its shape throughout indentation, though the indenter itself experienced at least 50 km of north-south directed Miocene shortening [*Schönborn*, 1999]. The Austroalpine crustal units north of the PF (grey shaded areas in Figure 7) are assumed to a first approximation to have behaved rigidly because by late Paleogene time their temperature was below 300°C [*Handy and Oberhänsli*, 2004; *Oberhänsli et al.*, 2004; *Schuster et al.*, 2004] marking the transition from viscous to brittle behavior in quartz-rich rocks [*Handy et al.*, 1999; *Stipp et al.*, 2002]. Any nonrigid behavior of the blocks is manifested in the model by gaps and overlaps between the blocks (see below). Units in the Tauern Window (Penninic nappes) and its frame (Lower Austroalpine; Figure 1) experienced temperatures greater than 300°C during indentation [*Luth and Willingshofer*, 2008] and were therefore ductile (red shaded areas), as reflected by their changing shapes and areas in map view in Figure 7.

The blocks in Figures 7a and 7b are separated by zones of deformation that accommodated most of the relative motion of these blocks as well as internal deformation of the blocks themselves. The white areas between

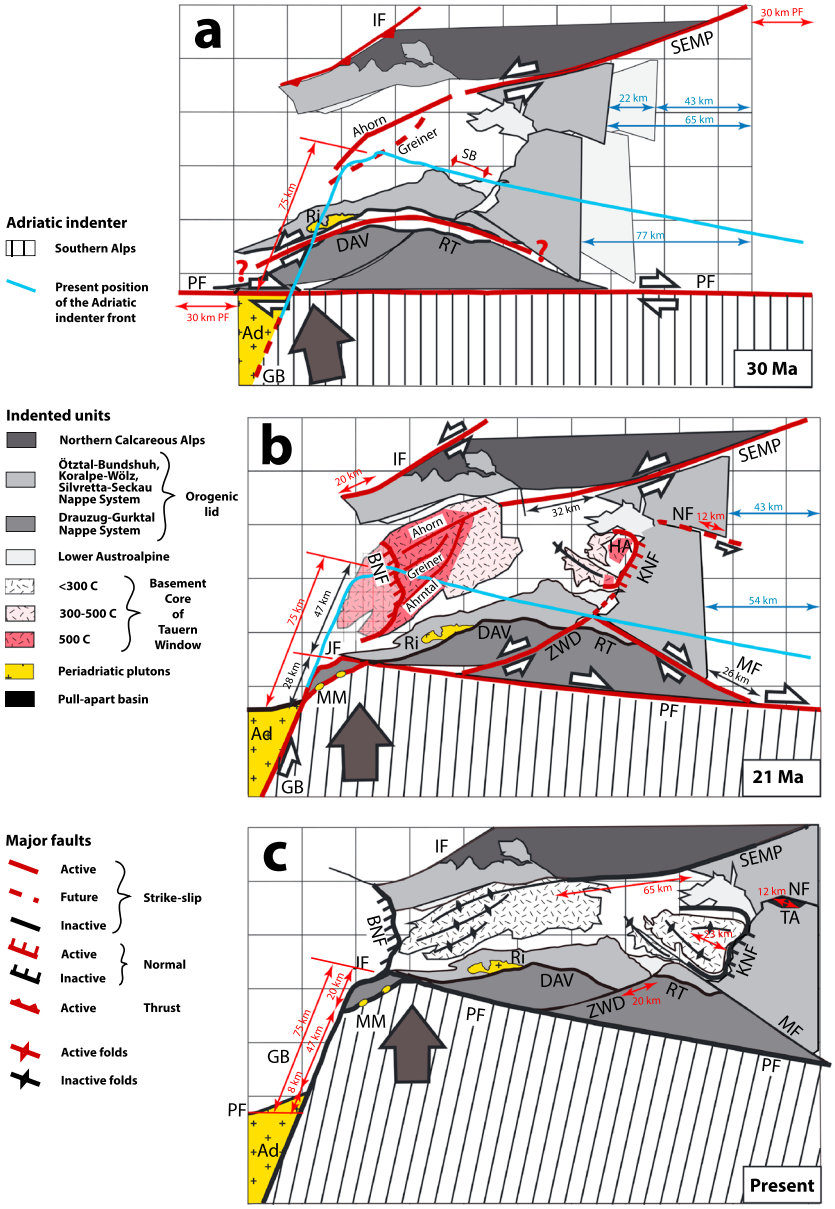

Figure 7. Map reconstructions of Adriatic indentation of the Eastern Alps in the Tauern Window area: (a) Initial exhumation during Periadriatic dextral strike-slip transpression and magmatism at 30 Ma. (b) Onset of indentation along the Giudicarie Belt at 21 Ma, initiation of rapid exhumation (doming and extensional unroofing) of Penninic units in the western Tauern Window, ongoing exhumation in the eastern Tauern Window due to northward motion of Austroalpine subindenters. (c) Present configuration as modified from map of *Schmid et al.* [2013]. Note that structures in the Tauern Window in Figures 7a and 7b were buried at 30 Ma and 23 Ma, respectively, and are projected to the surface at those times. The color shades indicate approximate temperature of buried crustal units: Red, 500°C; pink, 300°C; grey, <300°C. Folds and Domes: HA: Hochalm, SB: Sonnblick, Faults: BNF Brenner Normal Fault, DAV: Defferegen-Antholz-Vals Fault, GB: Giudicarie Belt, IF: Inntal Fault, JF: Jaufen Fault, KNF: Katschberg Normal Fault, MF: Mölltal Fault, MM: Meran-Mauls Fault, NF: Niedere Tauern Southern Fault, PF: Periadriatic Fault, RT: Ragga-Teuchel Fault, SEMP: Salzach-Ennstal-Mariazell-Puchberg Fault, ZWD: Zwischenbergen-Wöllatratten and Drautal Faults. Shear Zones: Ahorn, Greiner, and Ahrntal in Figures 7a and 7b mapped and dated by *Reicherter et al.* [1993], *Steffen et al.* [2001], and *Schneider et al.* [2013]. Periadriatic intrusive bodies: Ad: Adamello, Ri: Rieserferner. The arrows show lateral displacements: red: displacement constrained by offset structures, black: displacements obtained from rigid block motions and compatibility requirements, blue: amount of lateral escape resulting from displacements and block motions in the reconstructions. One square is 25 km to a side.

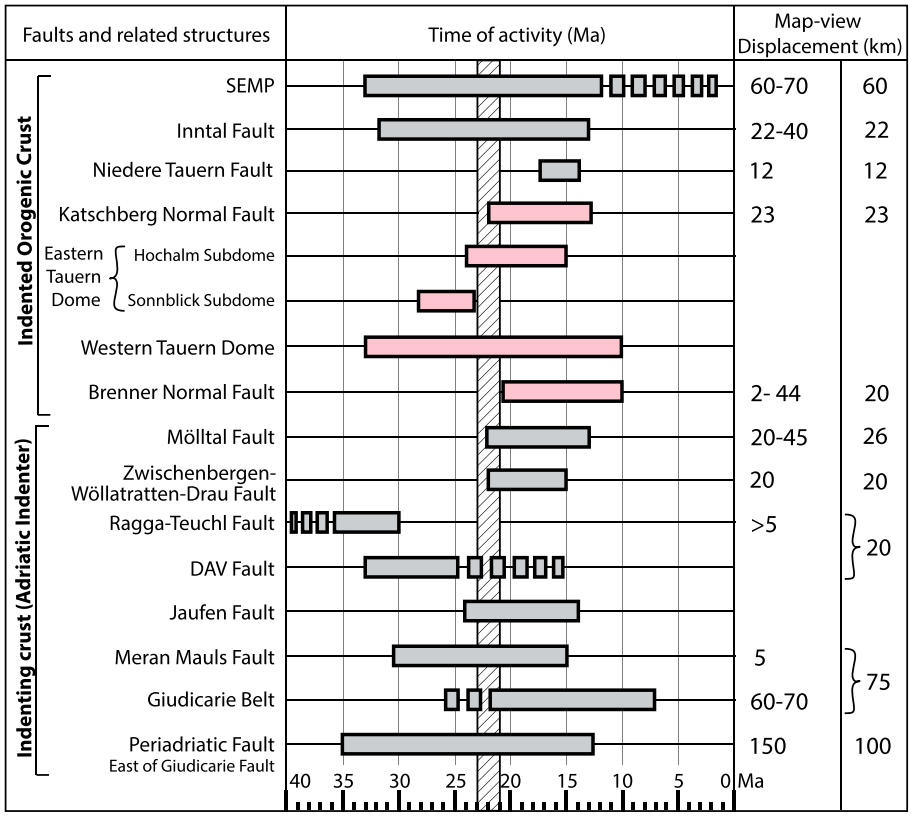

Figure 8. Age and displacement along main mylonitic (pink) and cataclastic (grey) faults involved in indentation. The bars and boxed dashes indicate probable and possible durations of fault activity, respectively. The vertical hatched bar marks the onset of the main phase of sinistral motion and indentation along the Giudicarie Fault (see text). SEMP Fault [*Frost et al.*, 2009; *Ratschbacher et al.*, 1991a, 1991b; *Frank*, 1987; *Peresson and Decker*, 1997a, 1997b; *Frisch et al.*, 1998; *Urbanek et al.*, 2002; *Linzer et al.*, 2002; *Glodny et al.*, 2008; *Schneider et al.*, 2013], Inntal Fault [*Decker et al.*, 1994; *Ortner and Sachsenhofer*, 1996; *Ortner*, 2003; *Ortner et al.*, 2006; *Linzer et al.*, 2002], Niedere Tauern Fault System [*Eder and Neubauer*, 2000; *Wölfler et al.*, 2011] and Tamsweg Basin [*Zeilinger*, 1997, *Zeilinger et al.*, 1999], Katschberg Normal Fault [*Liu et al.*, 2001; *Dunkl et al.*, 2003; *Scharf et al.*, 2013a, 2016], Hochalm Subdome [*Cliff et al.*, 1985; *Bertrand et al.*, 2013; *Scharf et al.*, 2013a; *Favaro et al.*, 2015], Sonnblick Subdome [*Inger and Cliff*, 1994; *Cliff et al.*, 1998, 2015; *Reddy et al.*, 1993; *Cliff and Meffan-Main*, 2003; *Favaro et al.*, 2015], Western Tauern Dome [*Satir*, 1975; *Thöni*, 1980; *von Blanckenburg et al.*, 1989; *Glodny et al.*, 2008; *Luth and Willingshofer*, 2008; *Schneider and Hammerschmidt*, 2009; *Kitzig*, 2010; *Pollington and Baxter*, 2010; *Rosenberg and Garcia*, 2011; *Schneider et al.*, 2013], Brenner Normal Fault [*Fügenschuh et al.*, 1997, 2012; *Frisch et al.*, 1998; *Glodny et al.*, 2008; *Rosenberg and Garcia*, 2011], Mölltal Fault [*Linzer et al.*, 2002; *Scharf et al.*, 2013a], Zwischenbergen-Wöllatratten-Drau Fault [*Scharf et al.*, 2013a], Ragga-Teuchl Fault [*Deutsch*, 1984; *Hoke*, 1990], DAV Fault [*Wagner et al.*, 2006; *Kleinschrodt*, 1987; *Borsi et al.*, 1979; *Schulz*, 1990; *Müller et al.*, 2000, 2001; *Mancktelow et al.*, 2001; *Most et al.*, 2003; *Romer and Siegesmund*, 2003; *Handy et al.*, 2005], Jaufen Fault [*Müller*, 1998, *Müller et al.*, 2001; *Viola et al.*, 2001; *Pomella et al.*, 2012], Meran-Mauls Fault [*Müller*, 1998, *Müller et al.*, 2001; *Prosser*, 1998; *Pomella et al.*, 2011, 2012], Giudicarie Belt [*Luciani*, 1989; *Elias*, 1998; *Müller et al.*, 2001; *Viola et al.*, 2001; *Pomella et al.*, 2011, 2012], and Periadriatic Fault [*Zwingmann and Mancktelow*, 2004; *Bögel*, 1975; *Scharbart*, 1975; *Laubscher*, 1988; *Läufer et al.*, 1997; *Frisch et al.*, 1998; *Müller*, 1998, *Müller et al.*, 2001; *Viola*, 2000; *Mancktelow et al.*, 2001; *Stipp et al.*, 2004; *Handy et al.*, 2005].

blocks signify gaps which correspond to domains of shortening (i.e., folding and shearing) when going forward in time. Conversely, overlaps correspond to areas of extension and/or erosional denudation going forward in time. The size of these gaps and overlaps, as well as the amount of displacement along intervening faults, is constrained by the age and displacement along these faults, as well as the thermal history of the area, as summarized in Figure 8 and discussed below. Of course, in kinematic reconstructions we strive to maintain compatibility by minimizing gaps and overlaps, but in practice, perfect compatibility is almost never realized due to the assumption that crustal blocks are rigid.

All crustal motions in Figure 7 are with respect to the top (northern) and left (western) sides of the grid which underlies the map. The only geological structure in Figure 7 that remains fixed with respect to this reference

frame is the Giudicarie Fault. This sinistral fault and its related thrust belt accommodated northward motion of the eastern Adriatic Indenter from ~21 to 7 Ma [e.g., *Pomella et al.*, 2012; *Handy et al.*, 2015, and references therein]. The present location of the leading edge of the Adriatic Indenter is marked in blue in Figures 7a–7c.

5.2. Time Slices of Map-View Restoration

Two main geologic considerations underlie our stepwise restoration of the Austroalpine subindenters and Tauern Window in Figure 7: The first concerns the shape of the Periadriatic Fault prior to indentation, which in this part of the Alps must have been fairly straight before 30 Ma [*Pomella et al.*, 2011] in order to accommodate an estimated 150 km of Paleogene oblique dextral strike-slip between the warm orogenic edifice and the cold Southern Alpine crust along the leading edge of the Adriatic Microplate [*Bögel*, 1975; *Laubscher*, 1988; *Schmid et al.*, 1989; *Handy et al.*, 2015] (see additional information in the supporting information). The age of this motion is constrained by Oligocene syntectonic granitoids (~32 Ma; Figures 1 and 7) [*Rosenberg*, 2004, and sources therein] as well as by 30–23 Ma cooling ages in Penninic nappes adjacent to the Periadriatic Fault in the central Alps [*Hurford*, 1986], where exhumation related to backfolding and –thrusting was broadly coeval with dextral motion on the Periadriatic Fault [*Schmid et al.*, 1987, 1989]. Of the total 150 km of this dextral motion, about 30 km was accommodated by transpression on the partly rotated Meran-Mauls Fault between 30 and 21 Ma, as shown in Figures 7a and 7b [*Ahrendt*, 1980; *Picotti et al.*, 1995; *Prosser*, 1998, 2000].

The second consideration concerns the amount and age of indentation along the sinistrally transpressive Giudicarie Belt. Total indentation is taken to be 75 km (Figure 7c) [*Laubscher*, 1988; *Ratschbacher et al.*, 1991b; *Werling*, 1992] based on cumulative offsets of the formerly continuous Periadriatic Fault (~50 km [*Castellarin et al.*, 2006]) and the dextrally transpressive Meran-Mauls Fault (28 km [*Pomella et al.*, 2012]). Indentation initiated along the Oligo-Miocene Meran-Mauls Fault (Figure 8) [*Müller et al.*, 2001; *Prosser*, 1998], which together with the Jaufen Fault (Figure 8), is interpreted to have formed a transpressional jog in the Periadriatic Fault by 21 Ma (Figure 7b) [*Pomella et al.*, 2011]. This early, minor phase of indentation offset and therefore postdated the Periadriatic intrusions preserved along the Meran-Mauls Fault [*Pomella et al.*, 2011]. The main phase of indentation is attributed to sinistral motion along the Giudicarie Belt (Figure 8) beginning no later than ~21 Ma (biostratigraphic dating of sediments beneath thrusts [*Luciani*, 1989; *Luciani and Silvestrini*, 1996 cited in *Scharf et al.*, 2013a; *Schmid et al.*, 2013]) and ending no later than 7 Ma (Messinian unconformity sealing thrusts [*Pieri and Groppi*, 1981; see *Handy et al.*, 2015]).

Thus, the role of the Periadriatic Fault changed fundamentally in late Oligocene-early Miocene time; beforehand, the PF was a dextral transpressive fault that extended continuously from the Western Alps to the Mid-Hungarian Fault System beneath the Pannonian Basin (Figure 1), whereas by 21 Ma, it was segmented, with the eastern part (east of the Giudicarie Fault) behaving as a stretching fault that accommodated eastward, orogen-parallel motion of the indented Eastern Alpine orogen, including the exhuming Penninic and Subpenninic units of the Tauern Window.

5.3. Quantifying Indentation, Orogenic Shortening, and Lateral Escape

A notable result of our reconstruction is that the amounts of indentation and lateral escape are roughly the same (70–75 km), within error, for the 30 Ma spanning Figures 7a–7c. We quantified horizontal shortening and extension by comparing the lengths of lines connecting Austroalpine and Southern Alpine units across (north-south) and Austroalpine units along (east-west) the Tauern Window in the three maps in Figure 7.

Initial north-south shortening (28 km) accommodated chiefly by the Meran-Mauls Fault. resulted in about 22 km of eastward lateral escape by 21 Ma (Figures 7a and 7b). Continued indentation of some 47 km during main activity of the sinistrally transpressive Giudicarie Belt between 21 Ma and the present induced about 43–54 km of lateral escape (Figures 7b and 7c). Most of the 71 km of lateral escape of the orogenic edifice (an average of the 65 and 77 km values given in Figure 7a) was accommodated by strike-slip faulting along the sinistral SEMP and the dextral Periadriatic faults; included in that amount are the 23 km of E-W extension taken up along the Katschberg Normal Fault [*Scharf et al.*, 2013a] together with its northern and southern mylonitic branches skirting the Eastern Tauern Dome. The Brenner Normal Fault is kinematically linked to the Western Tauern Dome in its footwall and along strike to the sinistral SEMP Fault. Together, the BNF and WTD acted as a bridge structure that transferred north-south motion on the Giudicarie Belt to east-west escape [*Scharf et al.*, 2013a] (Figures 1 and 7b).

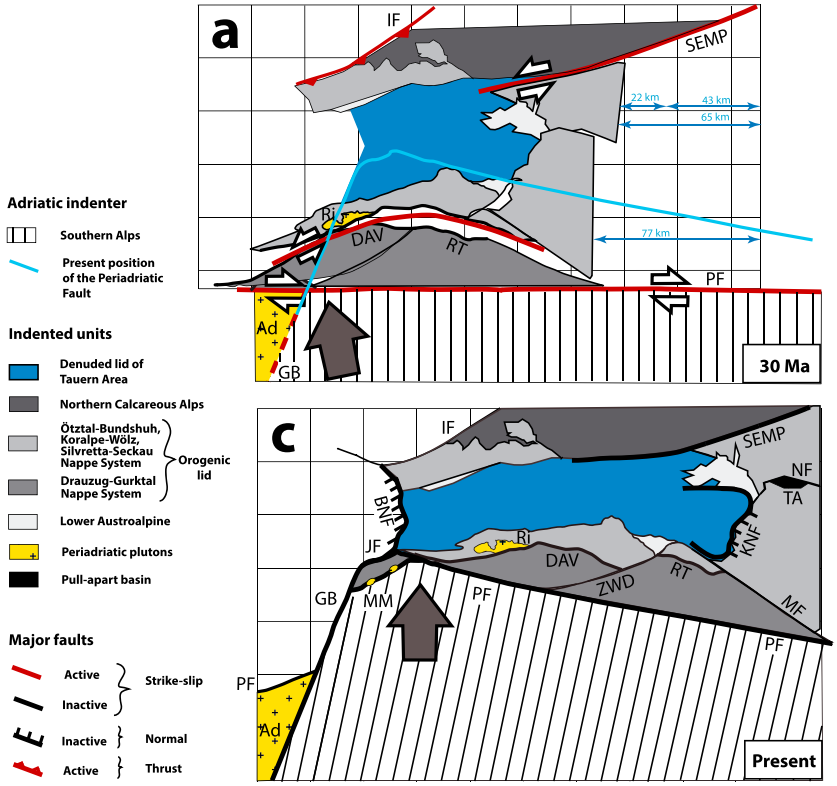

Figure 9. (a and c) Map reconstruction of Adriatic indentation of the Eastern Alps with blue areas showing denuded Penninic crust in the Tauern Window at 30 Ma and today, corresponding to maps in Figures 7a (top) and 7c (bottom). The blue line in Figure 9a indicates present front of the indenting Southern Alpine crust. Abbreviations as in Figures 1 and 7.

The style of deformation in the indented crust reflects its temperature and rheology during indentation; in the relatively cold (<300°C) Austroalpine units just north of the Periadriatic Fault, indentation lead to the formation of two triangular subindenters that deformed by a complex system of brittle, oblique-slip faults [*Linzer et al.*, 2002; *Scharf et al.*, 2013a; *Schuster et al.*, 2015], whereas in the warm Tauern Window (300–600°C), a system of upright folds and shear zones accommodated both vertical and horizontal motions [*Scharf et al.*, 2013a; *Schmid et al.*, 2013; *Schneider et al.*, 2013]. Shortening in the Tauern Window itself is not homogeneous, with more north-south shortening in the west (WTD, 25–30 km) than in the east (ETD, 11 km). We note that our estimate of north-south shortening for the WDT in Figure 7 is somewhat less than the 32 km estimate by *Schmid et al.* [2013] and far less than the 49 km of *Rosenberg and Berger* [2009]. This is partly due to the different location of cross sections and fold profiles used in their estimates, and partly to their use of line-balancing which yields an upper limit of horizontal shortening for the kilometer-scale, upright and tight-to-isoclinal folds in the Tauern Window; folding involved significant rotation and stretching of originally subhorizontal layering and nappe contacts subparallel to the subvertical axial planes.

Taken at face value, the approximate parity of north-south shortening and east-west extension suggests that there may have been little change in crustal thickness during indentation. However, this remains speculative in the absence of markers at depth in the Tauern Window area, e.g., the Moho, to indicate changes in crustal thickness through time.

5.4. Assessing the Relative Roles of Folding, Erosion, and Extensional Unroofing

Comparing the map-view areas of the Penninic and Subpenninic units in the reconstruction (blue areas in Figure 9) allows us to separate the denudational contributions in the Tauern Window of erosion, folding, and orogen-parallel extension since 30 Ma, and especially since the onset of pronounced indentation of the Eastern Alps at ~21 Ma. The blue area in Figure 9a (~3125 km^2) represents the area denuded without the contribution of post 23–21 Ma orogen-parallel extensional exhumation. This denudational area is therefore attributed to upright post-nappe folding and thickening which began sometime after the onset of

Adria-Europe collision and nappe formation at ~35 Ma but before the 30–25 Ma Tauernkristallisation (age references cited above).

The component of denudation that includes extensional unroofing is estimated by subtracting the blue area described above (~3125 km^2) and shown in Figure 9a from the blue area in the map for today in Figure 9c (~4375 km^2, ~5000 km^2 comprising the Lower Austroalpine units). This latter area includes denuded units affected by extensional shearing and continued upright folding for the period of 23–11 Ma in the footwalls of the oppositely dipping Brenner and Katschberg normal faults (Figure 9c). Thus, about two thirds of the denuded area in Figure 9c is attributable to erosion during north-south shortening and folding of the crust; only about a third of this areal denudation is due to tectonic unroofing in the footwalls of the Brenner and Katschberg normal faults.

Converting denuded area into denuded crustal volume requires assumptions about the thickness of the crustal lid above the Tauern area. Geobarometry yields peak pressures of 10–1.1 GPa [*Selverstone*, 1988; *Franz et al.*, 1991; *Kurz et al.*, 1998a, and references therein] and 0.75–0.8 GPa [*Dachs*, 1990; *Reddy*, 1990] for post-nappe Tauernkristallisation metamorphism, respectively, in the Western and Eastern Tauern domes. This metamorphism ranges in age from 30 to 25 Ma [*Oberhänsli et al.*, 2004, and references therein; *Pollington and Baxter*, 2010; *Favaro et al.*, 2015] and preceded the onset of rapid exhumation in the Tauern Window at about 23 Ma in the east [*Scharf et al.*, 2013a] and 20 Ma in the west [*Fügenschuh et al.*, 1997]. Thus, the peak pressures pertain to the thickened Tauern crust in Figure 9a prior to upright folding and extensional unroofing. For an average crustal density of 2.8 g/cm^3, the peak pressures place an upper bound of 38 km on the thickness of the denuded lid above the western part of the Tauern Window, corresponding to a volume of ~120.000 km^3 denuded since 30 Ma. An upper bound of about 28 km thickness and 87,000 km^3 for the denuded crust is obtained in a like manner for the eastern part of the Tauern Window, where post-nappe upright folds have lower amplitudes (cross sections in *Schmid et al.* [2013]). Minimum bounds on the thickness and volume of denuded crust (16 km, 70,000 km^3) are obtained by applying an orogenic geotherm of ~25 °C/km to the average 350–400°C temperature of upper greenschist-facies metamorphism [*Droop*, 1985] that prevailed in most of the Tauern Window (except the aforementioned domes) during the Tauernkristallisation.

The denuded crust from the Tauern area comprised Austroalpine crust as well as part of the Penninic and Subpenninic nappe pile according to detrital deposits with Tauern components in Oligo-Miocene clastics of the Inntal Basin (the so-called "Inntal Tertiary" [*Frisch et al.*, 2001]) and the northern Alpine Molasse Basin. After ~20 Ma, deposition shifted progressively to the Pannonian Basin [*Horváth et al.*, 2006] as drainage was channeled eastward by Miocene strike-slip faults accommodating crustal block rotation and eastward extrusion [*Frisch et al.*, 1998].

Our estimated denudational volume in the range of 70,000–120,000 km^3 for the Tauern source area overlaps with the 80,000 km^3 value estimated by *Kuhlemann et al.* [2001] from an analysis of Miocene sediment bodies in the northern Alpine Molasse Basin. *Kuhlemann et al.* [2001] generally lower volume reflects his use of the smallest denudational thickness (16 km) distributed over a larger area (5000 km^2) as derived from the reconstruction of *Frisch et al.* [1998], plus the fact that a significant amount of the sediment was also channeled into the Pannonian Basin. In contrast to our reconstruction in Figure 7, the *Frisch et al.* [1998] model assumes that the Austroalpine units on the eastern and western sides of the Tauern Window were contiguous before the onset of Miocene indentation, resulting in a much smaller proportion of fold-induced denudation (only 15,000 km^3 of the aforementioned total of 80,000 km^3 [*Kuhlemann et al.*, 2001]).

6. Conclusions

The structure evolution of fault-bounded blocks of Austroalpine crust along the front of the Adriatic Indenter had a major effect on the pattern of shortening and lateral escape of the orogenic crust in the Tauern Window. In the eastern part of the window, minor indentation beginning in late Oligo-Miocene time involved post-nappe upright folding that propagated away from the indenter front as indicated by the northeastward younging of mica cooling ages in the Venediger Nappe System [*Favaro et al.*, 2015]. The main phase of indentation starting no later than ~21 Ma lead to fragmentation of the Austroalpine subindenter, which was accommodated in the orogenic crust by continued upright folding and extensional exhumation in the

footwall of the laterally migrating Katschberg Normal Fault. The opposite shear sense of cataclasites along the indenter front (Mölltal Fault, dextral type 1 surfaces) and of adjacent mylonite along the southwestern margin of the Eastern Tauern Dome (sinistral ductile southern branch of the Katschberg Normal Fault) reflects the contrast in rheologies of the cold indenting block and hot, laterally extending and exhuming orogenic crust. By 17 Ma, the entire orogenic crust had cooled to below 300°C [*Dunkl et al.*, 2003; *Bertrand et al.*, 2015], resulting in brittle top-SE extension as recorded by fault surfaces in both the Austroalpine and Penninic units (cataclasite of the KNF and type 2 surfaces of the Mölltal Fault).

Similar patterns of indentation, folding, and orogen-parallel stretching are observed in the western Tauern Window where, however, north-south shortening was greater and kinematically linked to lateral escape along the sinistral SEMP Fault via a transpressional bridge structure in the Western Tauern Dome (Figures 7b and 7c) [*Scharf et al.*, 2013a]. This bridge structure, which after 21 Ma included the Brenner Normal Fault [*Fügenschuh et al.*, 1997], accommodated some 70 km of E-W extension.

Retrodeforming the post-nappe fold and fault systems of the Tauern Window in map view yields a 2-D reconstruction of the orogenic crust reaching back to 30 Ma (Figure 7). This model supports the notion that indentation lead to roughly equal amounts of north-south shortening (75 km) and east-west orogen-parallel stretching (71 km) of the orogenic crust in the Tauern Window. Estimates of the areas of denudation prior to and after the onset of indentation indicate that erosion associated with upright folding and thickening was the primary agent of denudation, whereas extensional unroofing accounted for only about a third of the total denudation and affected only the eastern and western ends of the Tauern Window in the footwalls of the Katschberg and Brenner normal faults.

Previous models of lateral escape and denudation in the Eastern Alps have tended either to emphasize the role of post-nappe, upright folding in the Tauern Window with only a small contribution of orogen-parallel extension [*Laubscher*, 1988; *Lammerer*, 1988; *Behrmann*, 1988; *Rosenberg et al.*, 2007; *Rosenberg and Garcia*, 2011, 2012] or, on the contrary, to assume orogen-parallel extension and unroofing to the virtual exclusion of doming [*Genser and Neubauer*, 1989; *Ratschbacher et al.*, 1991a, 1991b; *Frisch et al.*, 2000; *Linzer et al.*, 2002]. We follow *Fügenschuh et al.* [1997] in proposing a mix of coeval doming and orogen-parallel stretching of the Tauern Window in Miocene time but emphasize that the eastern and western parts of this window experienced different patterns of shortening and stretching: in the east, doming initiated before stretching and then migrated from SW to NE away from the indenter front [*Favaro et al.*, 2015], whereas in the west, strike-slip shearing preceded upright folding and this folding progressed from NW to SE toward the indenter [*Schneider et al.*, 2013].

These contrasting strain patterns may reflect varied structure of the interface between indenting and indented crust at depth. Gravimetry reveals a significant mass deficit in the vicinity of the western Tauern Window [*Ebbing et al.*, 2006], suggesting the existence of an anomalously dense body (~2.9 g/cm^3) that may be interpreted as an indenter within the underlying crust. A recent Moho study based on inverting the results of four independent geophysical methods (controlled-source seismology, ambient noise and local earthquake tomographies, and receiver functions) indicates that the Moho beneath the eastern half of the Tauern Window is poorly defined or even absent [*Spada et al.*, 2013]. Resolution of this problem is contingent on higher-resolution studies of crustal and mantle structure along the front of the Adriatic Indenter.

Acknowledgments
Special thanks go to our colleagues, Stefan Schmid, Claudio Rosenberg, Audrey Bertrand, and Susanne Schneider for many helpful discussions. Lazslo Fodor and Matteo Massironi gave us helpful tips on *P-T-B* analysis. We appreciate the remarks and comments of the two reviewers including (N. Mancktelow) and the editors. Interested readers can access supporting informaiton produced in this study and referred to in the text from mark. handy@fu-berlin.de. This study was supported partly by the German Science Foundation (DFG-project Ha 2403/10) in the form of a doctoral stipend and partly by unemployment benefits of the German government, both to the first author. The Geological Survey of Austria provide financial support for part of the field work. Finally, we appreciated the friendly assistance of Kathrin Aichorn and her team at the BIOS Center, Nationalpark Hohe Tauern in Austria where most of our field work was conducted.

References

Ahrendt, H. (1980), Die Bedeutung der Insubrischen Linie für den tektonischen Bau der Alpen, *N. Jb. Geol. Paläont. Abh.*, *160*, 336–362.
Argand, E. (1924), Des Alpes et de l'Afrique, *Bull. Soc. Vaud. Sci. Nat.*, *55*, 233–236.
Behrmann, J. H. (1988), Crustal-scale extension in a convergent orogen: The Sterzing–Steinach mylonite zone in the Eastern Alps, *Geodin. Acta*, *2*(2), 63–73.
Bertrand, A., C. Rosenberg, and S. Garcia (2015), Fault slip analysis and late exhumation of the Tauern Window, *Eastern Alps, Tectonophysics*, *649*, 1–17.
Borsi, S., A. Del Moro, F. P. Sassi, and G. Zirpoli (1979), On the age of the Vedrette di Ries (Rieserferner) massif and its geodynamic significance, *Geol. Rundsch.*, *68*(1), 41–60.
Bögel, H. (1975), Zur Literatur über die "Periadriatische Naht", *Verh. Geol. B.-A.*, *2-3*, 163–199.
Castellarin, A., G. B. Vai, and L. Cantelli (2006), The Alpine evolution of the Southern Alps around the Giudicarie faults: A Late Cretaceous to early Eocene transfer zone, *Tectonophysics*, *414*, 203–223.
Cliff, R. A., and S. Meffan-Main (2003), Evidence from Rb-Sr microsampling geochronology for the timing of Alpine deformation in the Sonnblick Dome, SE Tauern Window, Austria, in *Geochronology: Linking the Isotopic Record with Petrology and Textures*, edited by D. Vance, W. Müller, and I. M. Villa, *Geol. Soc. London, Spec. Publ.*, *220*, 159–172.

Cliff, R. A., G. T. R. Droop, and D. C. Rex (1985), Alpine metamorphism in the south-east Tauern Window, Austria: 2. Rates of heating, cooling and uplift, *J. Metam. Geol.*, *3*, 403–415.
Cliff, R. A., O. Oberli, and G. T. R. Droop (1998), Achieving geological precision in metamorphic geochronology: A Th-Pb age for the syn-metamorphic formation of the Mallnitzermulde Synform, Tauern Window, from individual allanite porphyroblasts, *J. Conf. Abstr. V.M. Goldschmidt Conf.*, *62A*, 337–338.
Cliff, R. A., F. Oberli, M. Meier, G. T. R. Droop, and M. Kelly (2015), Syn-metamorphic folding in the Tauern Window, Austria dated by Th-Pb ages from individual allanite porphyroblasts, *J. Metam. Geol.*, *33*, 427–435.
Dachs, E. (1990), Ceothermobarometry in metasediments of the southern Grossvenediger area (Tauern Window, Austria), *J. Metam. Geol.*, *8*, 217–230.
Dal Piaz, G. V. (1999), The Austroalpine-piedmont nappe stack and the puzzle of Alpine Tethys, *Sci. Geol. Mem.*, *51*(1), 155–176.
Davies, J. H., and F. von Blanckenburg (1995), Slab breakoff: A model of lithosphere detachment and its test in the magmatism and deformation of collisional orogens, *Earth Planet. Sci. Lett.*, *129*(1), 85–102.
Decker, K., H. Peresson, and P. Faupl (1994), Die miozäne Tektonik der östlichen Kalkalpen: Kinematik, Paläospannung und Deformationsaufteilung während der, lateralen Extrusion" der Zentralalpen", *Jahrb. Geol. Bundesanst.*, *137*, 5–18.
Delvaux, D., and B. Sperner (2003), Stress tensor inversion from fault kinematic indicators and focal mechanism data: The TENSOR program, in *New Insights into Structural Interpretation and Modelling*, edited by D. Nieuwland, *Geol. Soc. London, Spec. Publ.*, *212*, 75–100.
Deutsch, A. (1984), Young Alpine dykes south of the Tauern Window (Austria): A K-Ar and Sr isotope study, *Contrib. Mineral. Petrol.*, *85*, 45–57.
Droop, G. T. R. (1985), Alpine metamorphism in the south-east Tauern Window, Austria 1. P-T variations in space and time, *J. Metamorph. Geol.*, *3*, 371–402.
Dunkl, I., W. Frisch, and G. Grundmann (2003), Zircon fission track thermochronolgy of the southeastern part of the Tauern Window and adjacent Austroalpine margin, Eastern Alps, *Eclogae Geol. Helv.*, *96*, 209–217.
Ebbing, J., C. Braitenberg, and H.-J. Götze (2006), The lithospheric density structure of the Eastern Alps, *Tectonophysics*, *414*, 145–155.
Eder, N., and F. Neubauer (2000), On the edge of the extruding wedge: Neogene kinematics and geomorphology along the southern Niedere Tauern, Eastern Alps, *Eclogae Geol. Helv.*, *93*, 81–92.
Elias, J. (1998), The thermal history of the Ötztal–Stubai complex (Tyrol, Austria/Italy) in the light of the lateral extrusion model, *Tübinger Geowiss. Arb., Reihe A*, *42*, 1–172.
England, P., and P. Molnar (1990), Surface uplift, uplift of rocks, and exhumation of rocks, *Geology*, *18*, 1173–1177.
Exner, C. (1948), *Mallnitzer Rollfalte und Sirnfront des Sonnblick-Gneiskerns*, pp. 57–81, *Jahrbuch der Geologischen Bundesanstalt*, Wien.
Exner, C. (1964), *Erläuterungen zur Geologischen Karte der Sonnblickgruppe*, p. 130, *Geologische Bundesanstalt*, Wien.
Favaro, S., R. Schuster, M. R. Handy, A. Scharf, and G. Pestal (2015), Transition from orogen-perpendicular to orogen-parallel exhumation and cooling during crustal indentation—Key constraints from $^{147}Sm/^{144}Nd$ and $^{87}Rb/^{87}Sr$ geochronology (Tauern Window, Alps), *Tectonophysics*, *665*, 1–16.
Frank, W. (1987), Evolution of the Austroalpine elements in the Cretaceous, in *Geodynamics of the Eastern Alps*, edited by H. W. Flügel and P. Faupl, pp. 379–406, *Deuticke*, Wien.
Franz, G., V. Mosbrugger, and R. Menge (1991), Carbo-Permian pteridophyll leaf fragments from an amphibolite facies basement, Tauern Window, Austria, *Terra Nova*, *3*(2), 137–141.
Frisch, W., J. Kuhlemann, I. Dunkl, and A. Brügel (1998), Palinspastic reconstruction and topographic evolution of the Eastern Alps during late Cenozoic tectonic extrusion, *Tectonophysics*, *297*, 1–15.
Frisch, W., I. Dunkl, and J. Kuhlemann (2000), Post-collisional orgogen-parallel large-scale extension in the Eastern Alps, *Tectonophysics*, *327*, 239–265.
Frisch, W., J. Kuhlemann, I. Dunkl, and B. Szkely (2001), The Dachstein paleosurface and the Augenstein formation in the Northern Calcareous Alps—A mosaic stone in the geomorphological evolution of the Eastern Alps, *Int. J. Earth Sci.*, *90*, 500–518.
Frost, E., J. Dolan, C. Sammis, B. Hacker, J. Cole, and L. Ratschbacher (2009), Progressive strain localization in a major strike-slip fault exhumed from midseismogenic depths: Structural observations from the Salzach-EnnstalMariazel Puchberg fault system, Austria, *J. Geophys. Res.*, *114*, B04406, doi:10.1029/2008JB005763.
Fügenschuh, B., D. Seward, and N. S. Mantckelow (1997), Exhumation in a convergent orogen: The western Tauern Window, *Terra Nova*, *9*, 213–217.
Fügenschuh, B., N. S. Mancktelow, and S. S. Schmid (2012), Comment on Rosenberg and Garcia (2011): Estimating displacement along the Brenner fault and orogen-parallel extension in the Eastern Alps, International Journal of Earth Sciences, 100, 1129–1145, *Int. J. Earth Sci.*, *101*, 1451–1455, doi:10.1007/s00531-011-0725-4.
Genser, J., and F. Neubauer (1989), Low angle normal faults at the eastern margin of the Tauern window (Eastern Alps), *Mitt. Österr. Geol. Ges.*, *81*, 233–243.
Glodny, J., U. Ring, and A. Kühn (2008), Coeval high-pressure metamorphism, thrusting, strike-slip, and extensional shearing in the Tauern Window, Eastern Alps, *Tectonics*, *27*, TC4004, doi:10.1029/2007TC002193.
Handy, M. R., and R. Oberhänsli (2004), Metamorphic structure of the Alps, age map of the metamorphic structure of the Alps—Tectonic interpretation and outstanding problems, *Mitt. Österr. Geol. Ges.*, *149*, 201–226.
Handy, M. R., S. B. Wissing, and L. E. Streit (1999), Strength and structure of mylonite with combined frictional-viscous rheology and varied bimineralic composition, *Tectonophysics*, *303*(1), 175–192.
Handy, M. R., J. Babist, C. L. Rosenberg, R. Wagner, and M. Konrad (2005), Decoupling and is relation to strain partitioning in continental lithosphere—Insight from the Periadriatic fault system (European Alps), in *Deformation Mechanism, Rheology and Tectonics*, edited by D. Gapais, J. P. Brun, and P. R. Cobbold, *Geol. Soc. London, Spec. Publ.*, 243, 249–276.
Handy, M. R., S. M. Schmid, R. Bousquet, E. Kissling, and D. Bernoulli (2010), Reconciling plate-tectonic reconstructions of Alpine Tethys with the geological-geophysical record of spreading and subduction in the Alps, *Earth Sci. Rev.*, *102*, 121–158, doi:10.1016/j.earscirev.2010.06.002.
Handy, M. R., K. Ustaszewski, and E. Kissling (2015), Reconstructing the Alps–Carpathians–Dinarides as a key to understanding switches in subduction polarity, slab gaps and surface motion, *Int. J. Earth Sci.*, *104*(1), 1–26, doi:10.1007/s00531-014-1060-3.
Hoinkes, G., F. Koller, G. Rantitsch, E. Dachs, V. Hock, F. Neubauer, and R. Schuster (1999), Alpine metamorphism of the Eastern Alps, *Schweiz. Mineral. Petrogr. Mitt.*, *79*, 155–181.
Hoke, L. (1990), The Altkristallin of the Kreuzeck Mountains, SE Tauern Window, Eastern Alps-basement crust in a convergent plate boundary zone, *Jahrb. Geol. Bundesanst.*, *133*, 5–87.
Horváth, F., G. Bada, P. Szafián, G. Tari, A. Ádám, and S. Cloetingh (2006), Formation and deformation of the Pannonian basin: Constraints from observational data, in *European Lithosphere Dynamics*, edited by D. G. Gee, and R. A. Stephenson, *Geol. Soc. Lond. Mem.*, *32*, pp. 191–206.

Hurford, A. (1986), Cooling and uplift patterns in the Lepontine Alps South Central Switzerland and an age of vertical movement on the Insubric fault line, *Contrib. Mineral. Petrol.*, *92*(4), 413–427.
Inger, S., and R. A. Cliff (1994), Timing of metamorphism in the Tauern Window, Eastern Alps: Rb/Sr ages and fabric formation, *J. Metam. Geol.*, *12*, 695–707.
Johnson, M. R. E. (2002), Shortening budgets and the role of continental subduction during the India-Asia collision, *Earth Sci. Rev.*, *59*, 101–123.
Kitzig, M. C. (2010), Structural analyses and dating of deformation of the Ahrntal fault, MSc thesis, Freie Universität Berlin, Berlin, Germany.
Kleinschrodt, R. (1987), Quarzkorngefügeanalyse im Altkristallin südlich des westlichen Tauernfensters (Südtirol/Italien), *Erlanger Geol. Abh.*, *114*, 1–82.
Kuhlemann, J. (2000), Post-collisional sediment budget of circum-Alpine basins (Central Europe), *Mem. Sci. Geol. Padova*, *52*, 1–91.
Kuhlemann, J., W. Frisch, I. Dunkl, and B. Székely (2001), Quantifying tectonic versus erosive denudation by the sediment budget: The Miocene core complexes of the Alps, *Tectonophysics*, *330*, 1–23.
Kurz, W., and F. Neubauer (1996), Deformation partitioning during updoming of the Sonnblick area in the Tauern Window (Eastern Alps, Austria), *J. Struct. Geol.*, *18*(11), 1327–1343.
Kurz, W., F. Neubauer, H. Genser, and H. Horner (1994), Sequence of Tertiary brittle deformations in the eastern Tauem Window (Eastern Alps), *Mitt. Österr. geol. Ges.*, *86*, 153–164.
Kurz, W., F. Neubauer, and J. Genser (1996), Kinematics of Penninic nappes (Glockner nappe and basement-cover nappes) in the Tauern Window (Eastern Alps, Austria) during subduction and Penninic-Austroalpine collision, *Eclogae Geol. Helv.*, *89*(1), 573–605.
Kurz, W., F. Neubauer, and E. Dachs (1998), Eclogite meso- and microfabrics: Implications for the burial and exhumation history of eclogites in the Tauern Window (Eastern Alps) from P–T–d paths, *Tectonophysics*, *285*, 183–209.
Kurz, W., R. Handler, and C. Bertoldi (2008), Tracing the exhumation of the Eclogite zone (Tauern Window, Eastern Alps) by 40Ar/39Ar dating of white Mica in eclogites, *Swiss J. Geosci.*, *101*(1), 191–206, doi:10.1007/s00015-008-1281-1.
Lammerer, B. (1988), Thrust-regime and transpression-regime tectonics in the Tauern Window (Eastern Alps), *Geol. Rundsch.*, *77*(1), I43–156.
Laubscher, H. P. (1988), The arcs of the Western Alps and the northern Apennines: An updated view, *Tectonophysics*, *146*, 61–18.
Läufer, A. L., W. Frisch, G. Steinitz, and J. Loeschke (1997), Exhumed fault-bounded blocks along the Periadriatic lineament, *Geol. Rundsch.*, *86*, 612–626.
Linzer, H. G., K. Decker, H. Peresson, R. Dell'Mour, and W. Frisch (2002), Balancing lateral orogenic float of the Eastern Alps, *Tectonophysics*, *54*, 211–237.
Liu, Y., J. Genser, R. Handler, G. Friedl, and F. Neubauer (2001), $^{40}Ar/^{39}Ar$ muscovite ages from the Penninic-Austroalpine plate boundary, Eastern Alps, *Tectonics*, *20*, 526–547.
Luciani, V. (1989), Stratigrafia Sequenziale del Terziaro Nelle Catena del Monte Baldo (Provincie di Verona a Trento), *Sci. Geol. Mem.*, *41*, 263–351.
Luciani, V., and A. Silvestrini (1996), Planktonic foraminiferal biostratigraphy and paleoclimatology of the Oligocene/Miocene transition from the Monte Brione formation (northern Italy, Lake Garda), *Sci. Geol. Mem.*, *48*, 155–169.
Luth, S. W., and E. Willingshofer (2008), Mapping of the post-collisional cooling history of the eastern Apls, *Swiss J. Geosci.*, *101*, 207–223, doi:10.1007/s00015-008-1294-9.
Mancktelow, N. S., D. F. Stöckli, B. Grollimund, W. Müller, B. Fügenschuh, G. Viola, D. Seward, and I. M. Villa (2001), The DAV and Periadriatic fault systems in the Eastern Alps south of the Tauern window, *Int. J. Earth Sci.*, *90*, 593–622.
Marrett, R., and R. W. Allmendinger (1990), Kinematic analysis of fault-slip data, *J. Struct. Geol.*, *12*, 973–986.
Most, P., I. Dunkl, and W. Frisch (2003), Fission track tomography of the Tauern window along the TRANSALP profile, in *TRANSALP Conference*, edited by R. Nicolich, D. Polizzi, and S. Furlani, extended Abstracts, *Mem. Sci. Geol. Padova*, *54*, 225–226.
Müller, W. (1998), Isotopic dating of deformation using microsampling techniques: The evolution of the Periadriatic fault system (Alps), PhD thesis, ETH Zürich, 135 p.
Müller, W., N. S. Mancktelow, and M. Meier (2000), Rb-Sr microchrones of synkinematic mica in mylonites: An example from the DAV fault of the Eastern Alps, *Earth Planet. Sci. Lett.*, *180*, 385–397.
Müller, W., G. Prosser, N. S. Mancktelow, I. M. Villa, S. P. Kelley, G. Viola, and F. Oberli (2001), Geochronological constraints on the evolution of the Periadriatic fault system (Alps), *Int. J. Earth Sci.*, *90*, 623–653.
Oberhänsli, R., R. Bousquet, M. Engi, B. Goffé, G. Gosso, and M. Handy (2004), *Metamorphic Structure of the Alps 1:1000000*, *Commission for the Geological Map of the World*, Paris.
Ortner, H., and R. Sachsenhofer (1996), Evolution of the lower Inn Valley Tertiary and constraints on the development of the source area, in *Oil and Gas in Alpidic Thrustbelts and Basins of Central and Eastern Europe EAGE Special Publication*, vol. 5, edited by G. Wessely and W. Liebl, pp. 237–248, Geological Society, Londons.
Ortner, H. (2003), Local and far field stress-analysis of brittle deformation in the western part of the Northern Calcareous Alps, Austria, *Geol. Paläontol. Mitt. Univ. Innsbruck*, *26*, 109–131.
Ortner, H., F. Reiter, and R. Brandner (2006), Kinematics of the Inntal shear zone–sub-Tauern ramp fault system and the interpretation of the TRANSALP seismic section, Eastern Alps, Austria, *Tectonophysics*, *414*, 241–258.
Peresson, H., and K. Decker (1997a), Far-field effects of late Miocene subduction in the Eastern Carpathians: E–W compression and inversion of structures in the Alpine-Carpathian–Pannonian region, *Tectonics*, *16*, 38–56.
Peresson, H., and K. Decker (1997b), The Tertiary dynamics of the northern Eastern Alps (Austria): Changing paleostresses in a collisional plate boundary, *Tectonophysics*, *272*, 125–157.
Pestal, G., E. Hejl, R. Braunstingl, and R. Schuster (2009), *Erläuterungen zur Geologischen Karte von Salzburg 1:200.000*, pp. 491–502, Geologische Bundesanstalt, Wien.
Petit, J. P. (1987), Criteria for sense of movement on fault surfaces in brittle rocks, *J. Struct. Geol.*, *9*(5/6), 597–608.
Picotti, V., G. Prosser, and A. Castellarin (1995), Structures and kinematics of the Giudicarie - Val Trompia fold and thrust belt (central Southern Alps northern Italy), *Mem. Sc. Geol*, *47*, 95–109.
Pieri, M., and G. Groppi (1981), Subsurface geological structures of the Po Plain. CNR-PF Geodinamica, Sottoprog. Modello Strutturale contr. 414.
Pollington, A. D., and E. Baxter (2010), High resolution Sm-Nd garnet geochronology reveals the uneven pace of tectonometamorphic processes, *Earth Planet. Sci. Lett.*, *293*, 63–71.
Pomella, H., U. Klötzli, R. Scholger, M. Stipp, and B. Fügenschuh (2011), The northern Giudicarie and the Meran-Mauls fault (Alps, northern Italy) in the light of new paleomagnetic and geochronological data from boudinaged Eo−/Oligocene tonalites, *Int. J. Earth Sci.*, *100*, 1827–1850, doi:10.1007/s00531-010-0612-4.
Pomella, H., M. Stipp, and B. Fügenschuh (2012), Thermochronological record of thrusting and strike-slip faulting along the Giudicarie fault system (Alps, northern Italy), *Tectonophysics*, *579*, 118–130, doi:10.1016/j.tecto.2012.04.015.

Prosser, G. (1998), Strike-slip movements and thrusting along a transpressive fault zone: The North Giudicarie line (Insubric line, northern Italy), *Tectonics*, *17*(6), 921–937.
Prosser, G. (2000), The development of the North Giudicarie fault zone (Insubric line, northern Italy), *J. Geodyn.*, *30*(1–2), 229–250.
Ratschbacher, L., O. Merle, P. Davy, and P. Cobbold (1991a), Lateral extrusion in the eastern Alps, Part1: Boundary conditions and experiments scaled for gravity, *Tectonics*, *10*, 245–256.
Ratschbacher, L., W. Frisch, H. G. Linzer, and O. Merle (1991b), Lateral extrusion in the Eastern Alps, Part2: Structural analysis, *Tectonics*, *10*, 257–271.
Reddy, S. M. (1990), The structural, metamorphic and thermal history of the Sonnblick Dome, southeast Tauern Window, Austria (Doctoral dissertation, University of Leeds).
Reddy, S. M., R. A. Cliff, and R. East (1993), Thermal history of the Sonnblick Subdome, south-east Tauern Window, Austria: Implications for heterogeneous uplift within the Pennine basement, *Geol. Rundsch.*, *82*, 667–675.
Reicherter, K., R. Fimmel, and W. Frisch (1993), Sinistral strike-slip faults in the central Tauern window (Eastern Alps, Austria), *Jahrb. Geol. Bundesanst.*, *136*, 495–502.
Romer, R. L., and S. Siegesmund (2003), Why allanite may swindle about its true age, *Contrib. Mineral. Petrol.*, *146*, 297–307.
Rosenberg, C. L. (2004), Shear zones and magma ascent: A model based on a review of the Tertiary magmatism in the Alps, *Tectonics*, *23*, TC3002, doi:10.1029/2003TC001526.
Rosenberg, C. L., and A. Berger (2009), On the causes and modes of exhumation and lateral growth of the Alps, *Tectonics*, *28*, TC6001, doi:10.1029/2008TC002442.
Rosenberg, C. L., and S. Garcia (2011), Estimating displacement along the Brenner fault and orogen-parallel extension in the Eastern Alps, *Int. J. Earth Sci.*, *100*, 1129–1145.
Rosenberg, C. L., and S. Garcia (2012), Reply to the comment of Fügenschuh et al. on the paper 'Estimating displacement along the Brenner fault and orogen-parallel extension in the Eastern Alps' by Rosenberg and Garcia, Int J Earth Sci (2011) 100:1129–1145, *Int. J. Earth Sci.*, *101*, 1457–1464, doi:10.1007/s00531-011-0726-3.
Rosenberg, C. L., and E. Kissling (2013), Three-dimensional insight into central-Alpine collision: Lower-plate or upper-plate indentation?, *Geology*, *41*, 1219–1222, doi:10.1130/G34584.1.
Rosenberg, C. L., J. P. Brun, F. Cagnard, and D. Gapais (2007), Oblique indentation in the Eastern Alps: Insights from laboratory experiments, *Tectonics*, *26*, TC2003, doi:10.1029/2006TC001960.
Sander, B. (1911), Geologische Studien am Westende der hohen Tauern. Bericht—Denkschrift d. kais, *Akademie der Wissenschaften*, *83*, 257–319.
Satir, M. (1975), Die Entwicklungsgeschichte der westlichen Hohen Tauern und der südlichen Ötztalmasse auf Grund radiometrischer Altersbestimmungen, PhD thesis, Società cooperativa tipografica, Padova, 1–84.
Scharbart, S. (1975), Radiometrische Altersdaten von Intrusivgesteinen im Raum Eisenkappel (Karawanken, K~irnten), *Verh. Geol. Bundesanst.*, *4*, 301–304.
Scharf, A., M. R. Handy, S. Favaro, S. M. Schmid, and A. Bertrand (2013a), Modes of orogen-parallel stretching and extensional exhumation of thickening orogenic crust in response to microplate indentation and slab roll-back (Tauern Window, Eastern Alps), *Int. J. Earth Sci.*, *102*(6), 1627–1654, doi:10.1007/s00531-013-0894-4.
Scharf, A., M. R. Handy, M. A. Ziemann, and S. M. Schmid (2013b), Peak-temperature patterns of polyphase metamorphism resulting from accretion, subduction and collision (eastern Tauern Window, European Alps)—A study with Raman microspectroscopy on carbonaceous material (RSCM), *J. Metam. Geol.*, *31*(8), 863–880, doi:10.1111/jmg.12048.
Scharf, A., M. R. Handy, S. M. Schmid, S. Favaro, M. Sudo, R. Schuster, and K. Hammerschmidt (2016), Grain-size effects on the closure temperature of white mica in a crustal-scale extensional shear zone – Implications for dating shearing and cooling from in-situ $^{40}Ar/^{39}Ar$ laser-ablation ages of white mica (Tauern Window, Eastern Alps), *Tectonophysics*, *674*, 210–226, doi:10.1016/j.tecto.2016.02.014.
Schmid, S. M., A. Zingg, and M. R. Handy (1987), The kinematics of movements along the Insubric line and the emplacement of the Ivrea zone, *Tectonophysics*, *135*, 47–66.
Schmid, S. M., H. R. Aebli, F. Heller, and A. Zingg (1989), The role of the Periadriatic line in the tectonic evolution of the Alps, in *Alpine Tectonics*, edited by M. P. Coward, D. Dietrich, and R. Park, *Geol. Soc. London, Spec. Publ.*, *45*, 153–171.
Schmid, S. M., B. Fügenschuh, E. Kissling, and R. Schuster (2004), Tectonic map and overall architecture of the Alpine orogen, *Eclogae Geol. Helv.*, *97*, 93–117, doi:10.1007/s00015-004-1113-x.
Schmid, S. M., A. Scharf, M. R. Handy, and C. L. Rosenberg (2013), The Tauern Window (Eastern Alps, Austria) – A new tectonic map, cross-sections and tectonometamorphic synthesis, *Swiss J. Geosci.*, *106*, 1–32, doi:10.1007/s00015-013-0123-y.
Schneider, S. and K. Hammerschmidt (2009), K-Ar dating of sinistral deformation in the upper Schieferhülle, south-western Tauern Window (Eastern Alps), *EGU General Assembly Conference Abstracts*, 11, 13813.
Schneider, S., K. Hammerschmidt, and C. L. Rosenberg (2013), Dating the longevity of ductile shear zones: Insight from $^{40}Ar/^{39}Ar$ in situ analyses, *Earth Planet. Sci. Lett.*, *369-370*, 43–58, doi:10.1016/j.epsl.2013.03.002.
Schönborn, G. (1999), Balancing cross sections with kinematic constraints: The dolomites (northern Italy), *Tectonics*, *18*(3), 527–545.
Schulz, B. (1990), Prograde-retrograde P-T-t-deformation path of Austroalpine micaschists during Variscan continental collision (Eastern Alps), *J. Metam. Geol.*, *8*, 629–443.
Schuster, R., F. Koller, V. Hoeck, G. Hoinkes, and R. Bousquet (2004), Explanatory notes to the map: Metamorphic structure of the Alps-metamorphic evolution of the Eastern Alps, *Mitt. Österr. Geol. Ges.*, *149*, 175–199.
Schuster, R., P. Tropper, E. Krenn, F. Finger, W. Frank, and R. Philippitsch (2015), Prograde Permo-Triassic metamorphic HT/LP assemblages from the Austroalpine Jenig complex (Carinthia, Austria), *Aust. J. Earth Sci.*, *108*(1), 73–90, doi:10.17738/ajes.2015.0005.
Selverstone, J. (1988), Evidence for east-west crustal extension in the Eastern Alps: Implications for the unroofing history of the Tauern Window, *Tectonics*, *7*, 87–105.
Selverstone, J. (2004), Are the Alps collapsing?, *Annu. Rev. Earth Planet. Sci.*, *33*(1), 113–132, doi:10.1146/annurev.earth.33.092203.122535.
Spada, M., I. Bianchi, E. Kissling, N. Piana Agostinetti, and S. Wiemers (2013), Combining controlled-source seismology and receiver function information to derive 3-D Moho topography for Italy, *Geophys. J. Int.*, *194*(2), 1050–1068, doi:10.1093/gji/ggt148.
Steffen, K., J. Selverstone, and A. Brearley (2001), Episodic weakening and strengthening during synmetamorphic deformation in a deep crustal shear zone in the Alps, *Geol. Soc. London Spec. Publ.*, *186*, 141–156.
Stipp, M., H. Stünitz, R. Heilbronner, and S. M. Schmid (2002), The eastern Tonale fault zone: A natural laboratory for crystal plastic deformation of quartz over a temperature range from 250 to 700°C, *J. Struct. Geol.*, *24*, 1861–1884.
Stipp, M., B. Fügenschuh, L. P. Gromet, H. Stünitz, and S. M. Schmid (2004), Contemporaneous plutonism and strike-slip faulting: A case study from the Tonale fault zone north of the Adamello pluton (Italian Alps), *Tectonics*, *23*, TC3004, doi:10.1029/2003TC001515.

Tapponnier, P., G. Peltzer, and R. Armijo (1986), On the mechanics of the collision between India and Asia, in *Collision Tectonics*, edited by M. P. Coward and A. C. Ries, *Geol. Soc. London Spec. Publ.*, *19*, 113–157.

Thöni, M. (1980), Distribution of pre-Alpine and Alpine metamorphism of the southern Ötztal mass and the Scarl unit based on K/Ar age determinations, *Mitt. Österr. Geol. Ges.*, *71*, 139–165.

Urbanek, C., W. Frank, B. Grasemann and K. Decker (2002), Eoalpine versus Tertiary deformation: Dating of heterogeneously partitioned strain (Tauern Window, Austria). Pangeo Austria: Erdwissenschaften in Österreich 28.-30.6.2002 (Program and abstract), Institute for geology and paleontology University of Salzburg.

Viola, G. (2000), Kinematics and timing of the Periadriatic fault system in the Giudicarie region (central-Eastern Alps), PhD thesis, University of Zurich.

Viola, G., N. S. Mancktelow, and D. Seward (2001), Late Oligocene-Neogene evolution of Europe-Adria collision: New structural and geochronological evidence from the Giudicarie fault system (Italian Eastern Alps), *Tectonics*, *20*(6), 999–1020.

von Blanckenburg, F., I. M. Villa, H. Baur, G. Morteani, and R. H. Steiger (1989), Time calibration of a PT-path from the western Tauern window, eastern Alps: The problem of closure temperatures, *Contrib. Mineral. Petrol.*, *101*, 1–11.

Wagner, R., C. L. Rosenberg, M. R. Handy, C. Möbus, and M. Abertz (2006), Fracture-driven intrusion and upwelling of a mid-crust pluton fed from a transpressive shear zone—The Rieserferner pluton (Eastern Alps), *Geol. Soc. Am. Bull.*, *118*(1–2), 219–237, doi:10.1130/B25841.1.

Werling, E. (1992), Tonale-, Pejo- und Judicarien-Linie: Kinematik, Mikrostrukturen und Metamorphose von Tektoniten aus räumlich interferierenden aber verschiedenaltrigen Verwerfungszonen, PhD thesis, ETH Zurich.

Wölfler, A., W. Kurz, H. Fitz, and K. Stüwe (2011), Lateral extrusion in the Eastern Alps revisited: Refining the model by thermochronological, sedimentary, and seismic data, *Tectonics*, *30*, TC4006, doi:10.1029/2010TC002782.

Zeilinger, G. (1997), Das Tamsweger Tertiär: Fazies und Deformation eines intramontanen Beckens und seine regionale geodynamische Bedeutung, Diploma Thesis at University Tübingen.

Zeilinger, G., J. Kuhlemann, J. Reinecker, M. Kàzmer, and W. Frisch (1999), Das Tamsweger Tertiär im Lungau (Österreich): Fazies und Deformation eines intramontanen Beckens und seine regionale geodynamische Bedeutung, *Neues Jahrb. Geol. Palaontol. Abh.*, *214*(3), 537–568.

Zwingmann, H., and N. Mancktelow (2004), Timing of Alpine fault gouges, *Earth Planet. Sci. Lett.*, *223*, 415–425.